Deanship of Graduate Studies
Al-Quds University

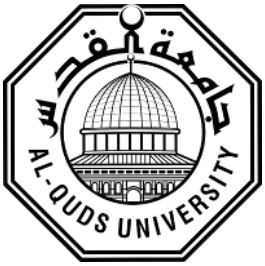

Contributions on Fading Channel Estimation for 5G Mobile Systems

Moataz Hussein Ali Qaroush

M.Sc. Thesis

Jerusalem-Palestine

1440-2018

Contributions on Fading Channel Estimation for 5G Mobile Systems

Prepared By:

Moataz Hussein Ali Qaroush

B.Sc.: Electrical Engineering/Birziet

University-Palestine

Supervisor: Dr. Ali Jamoos

A thesis submitted in partial fulfillment of the requirements for the degree of Master of Electronic and Computer Engineering/Department of Electronic and Computer Engineering/ Faculty of Engineering/ Graduate Studies

Jerusalem-Palestine

1440-2018

Al-Quds University

Deanship of Graduate Studies

Electronics and Computer Engineering

Faculty of Engineering

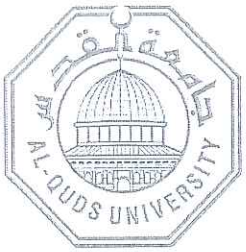

Thesis Approval

Contributions on Fading Channel Estimation for 5G Mobile Systems

Prepared By: Moataz Hussein Ali Qaroush

Registration No: 21411608

Supervisor: Dr. Ali Jamoos

Master thesis submitted and accepted, Date: 18/12/2018

The name and signatures of examining committee members are as follows:

1- Head of the committee	Dr. Ali Jamoos	Signature: .....
2- Internal Examiner	Dr. Ahmed Abdou	Signature: .....
3- External Examiner	Dr. Murad abu Subaih	Signature: .....

Jerusalem-Palestine

1440-2018

Declaration

I certify that this thesis submitted for the degree of Master, is the result of my own research, except where otherwise acknowledged, and that this study (or any part of the same) has not been submitted for a higher degree to any other university or institution.

Signed by: .....

Moataz Hussein Ali Qaroush

Date: 18/12/2018

Acknowledgments

I would like to bless my God for everything.

I would like to express my deepest gratefulness to my family especially my parents, my wife, my children for the endless care they have provided advice, support, patience, and me.

Special thanks go out to my supervisor, Dr. Ali Jamoos, whose give me more knowledge and skills in the communication field. In addition, his guidance helped me in all the time of research and writing of this thesis.

My sincere thanks also go to the electronics and computer department at Al-Quds University for helping me in topics that are related to digital signal processing.

I would like to express my thanks to president of Al-Quds Open University Prof. Younes Amro and President Assistant for technology and production at Al-Quds Open University Dr. Islam Amro for their encouragement to complete higher education.

I would like to express my thankfulness to all those who helped me during the period of my study and give me motivation and encouragement.

Abstract

Universal filtered multi-carrier (UFMC) modulation is a very powerful candidate to be employed for future 5G mobile systems. It overcomes the limitations and restrictions in current modulation techniques employed in 4G mobile systems such as orthogonal frequency division multiplexing (OFDM) and Filter bank multicarrier (FBMC). In addition, UFMC can support future applications like machine-to-machine (M2M), device-to-device (D2D), and vehicle-to-vehicle (V2V) communications.

In this thesis, we address the estimation of UFMC fading channels based on the comb-type pilot arrangement in the frequency domain. The basic solution is to estimate the fading channel based on the mean square error (MSE) or least square (LS) criteria with adaptive implementation using least mean square (LMS) or recursive least square (RLS) algorithms. However, these adaptive filters seem not effective, as they cannot fully exploit fading channel statistics. To take advantage of these statistics, the time-variations of the fading channel is modelled by an autoregressive process (AR) and tracked by an H_∞ filter. Nevertheless, this requires the AR model parameters, which are estimated by solving the Yule-Walker equation (YWE), based on the Bessel autocorrelation function (ACF) of the fading channel with known Doppler rate.

The results of MATLAB simulations show the effectiveness of the proposed H_∞ filter based channel estimator as compared with Kalman filter, and conventional adaptive filters such as RLS and LMS algorithms. Furthermore, the low pass interpolation is confirmed to outperform both spline and linear interpolation.

Keywords: fading channel, channel estimation, autoregressive model, 5G, UFMC, H_∞ filter, Kalman filter, LMS Filter, RLS Filter.

Table of Contents

List of Figures

Chapter 1

Introduction

In wireless communication systems, 1G refers to the first generation of the mobile wireless communication system. To this date, there are main fourth mobile generation named (1G-4G). Since 1G was introduced in the early 1979s, a new wireless mobile telecommunications technology has been released roughly every 10 years. All of them refer to the technology used by the mobile carrier and device itself. They have different speeds and features that improve on the previous generation. The next generation is 5G, which is scheduled to launch in 2020-2030.

1.1 Evolution of Mobile Generation

1.1.1 Zero Generation (0G)

0G is also known as mobile radio telephone systems. It was invented before 1979. This system was analog in nature. Generally, 0G provides half-duplex communications. These mobile telephones were placed in ships, trains and vehicles. In addition, it was very costly [1].

1.1.2 First Generation (1G)

In 1979, the first mobile generation (1G) was launched. The main growth that differentiated the 1G from the previous generation was the use of multiple cell sites and the capability to move calls from one site to the next as the user moved between cells during a conversation [1]. Each base station (cell site) supporting service to a specific area (cell). The cell sites would be set up such that cells partially overlapped. In a cellular system, a signal between a base station (cell site) and a terminal (phone) only require be strong enough to reach between them, so the same channel can be employed simultaneously for individual conversations in another cells.

1.1.3 Second Generation (2G)

In the1990s, the second generation (2G) mobile phone systems was launched. The main difference of the 2G from the previous generation was the use of digital transmission instead of analog transmission. The rise in mobile phone usage as a result of 2G was explosive and this era also saw the advent of prepaid mobile phones. The 2G introduced a new different to communication, as SMS text messaging became possible, initially on GSM networks and eventually on all digital networks [1-2]. Several advantages of 2G were digital signals need use less battery power, so it betters mobile batteries to keep long. Digital coding betters the voice clarity and decreases noise in the line. Digital encryption has granted secrecy and safety to the data and voice calls.

1.1.4 Third generation (3G)

3G was launched in 2000. As the usage of 2G phones became more widespread and people began to use mobile phones in their daily lives, it became clear that demand for data services

like web browsing, sending emails, media streaming and stream radio was growing. The major technological difference that distinguishes 3G technology from 2G technology is the use of packet switching rather than circuit switching for data transmission [3].

1.1.5 Fourth generation (4G)

4G is the current mobile generation. It is basically the expansion in the 3G technology with more bandwidth and services offers in the 3G. The main service for the 4G technology is high quality audio/video streaming over end to end internet protocol [4]. One of the major ways in which 4G differed technologically from 3G was employing an all internet protocol network instead of circuit switching.

1.1.6 Fifth Generation (5G)

5G is the fifth generation of cellular mobile communication, offering high data rate, faster speeds, higher connection density, energy saving. 5G development is under research, 5G networks are expected to launch across the world by 2020-2030.

Table (1.1) summarizes the main differences between the mobile generations (1G to 5G) in a wireless communication system [5].

Table 1. 1: Comparison of 1G to 5G technology [5]

Technology	**1G**	**2G**	**2.5G**	**3G**	**4G**	**5G**
Period	1980-1990	1990-2000	1995	2000-2010	2010-2020	2020-2030
Services	Analog Voice	Digital Voice, Short messages	Higher Capacity, Packetized Data	Higher Capacity broadband data 2Mbps	Higher Capacity complementary IP-Oriented, Multimedia Data	Dynamic information access, Wearable devices
Standards	AMPS TACS NMT	TDMA CDMA GSM	GPRS EDGE 1xRTT	WCDMA CDMA2000 UMTS	LTE WIFI WiMAX	WWWW

		PDC				
Data Rate	1.9Kbps	14.4Kbps	384Kbps	2Mbps	200Mbps	1Gbps-10Gbps
Bandwidth	900MHz	900MHz	100MHz	100MHz	100MHz	-
Channel Band width	30KHz	200Khz	200Khz	5Mhz	200Mhz	
Multiplexing	FDMA	TDMA CDMA	TDMA CDMA	CDMA	OFDMA	
Core Network	PSTN	PSTN	PSTN, Packet Network	Packet Network	Internet	Internet
Handover	Horizontal	Horizontal	Horizontal	Horizontal	Horizontal And Vertical	Horizontal And Vertical

1.2 **Global Mobile Data Traffic Forecast Update**

In this section, we will introduce some figures for mobile data traffic and growth of owned smart devices. Figures (1.1, 1.2) [6], shows the growth of a number of smart devices between (2005-2013). In Peter's square in 2005 when Pope greeted the public, we notice a few persons had a smartphone. While in 2013 for the same occasion in Peter's square, most of the people have owned smartphones, which clearly shows that there is an increasing number of owned devices and connected devices to the internet in the future.

Figure 1. 1: The number of Smartphones in 2005 [6]

Figure 1. 2: The growth of the number of Smartphones in 2013 [6]

Figure (1.3) shows the expectation of growing traffic to (49) Exabyte per month at 2021, while the data traffic was (7) Exabyte at 2016 [7].

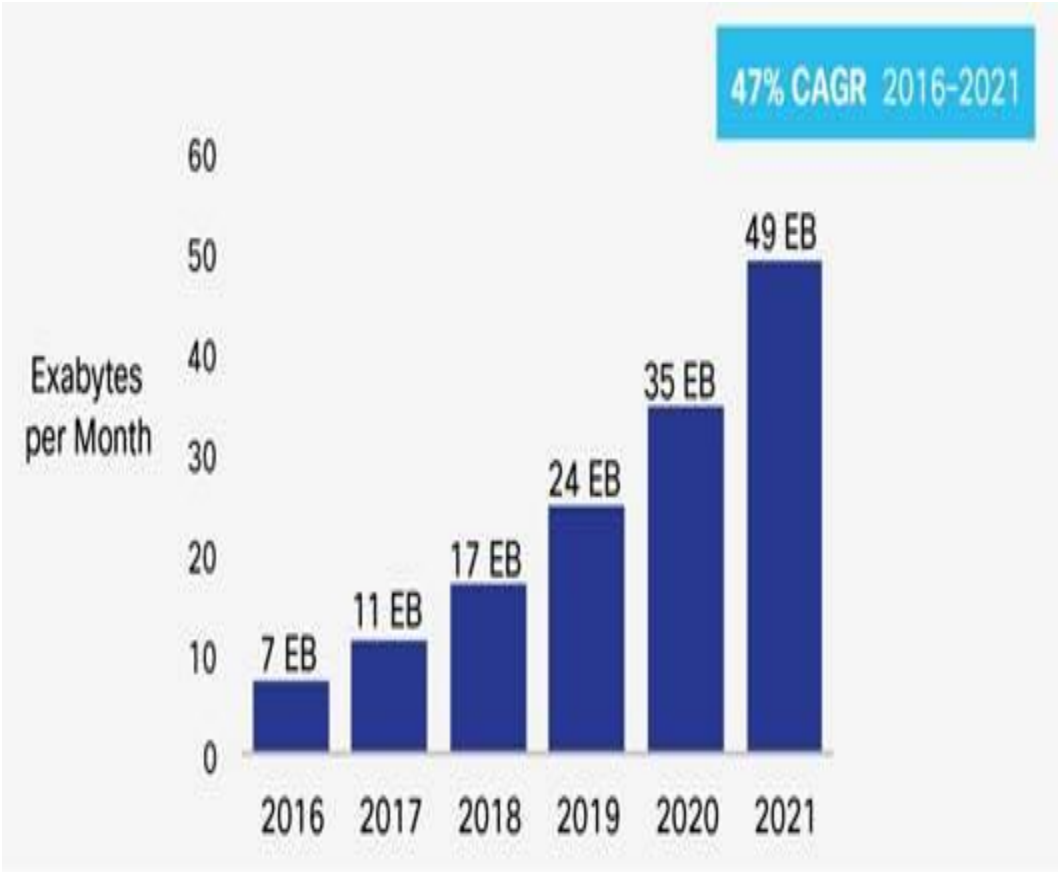

Figure 1. 3: Growth of Traffic between (2016 and 2021) [7]

Figure (1.4) shows cisco estimated mobile video traffic between 2016 and 2021. While mobile video represented more than half of global mobile data traffic beginning at 2012, the

report predicts that (38) Exabytes from total (49) Exabytes per month crossing mobile network will be due to video [7].

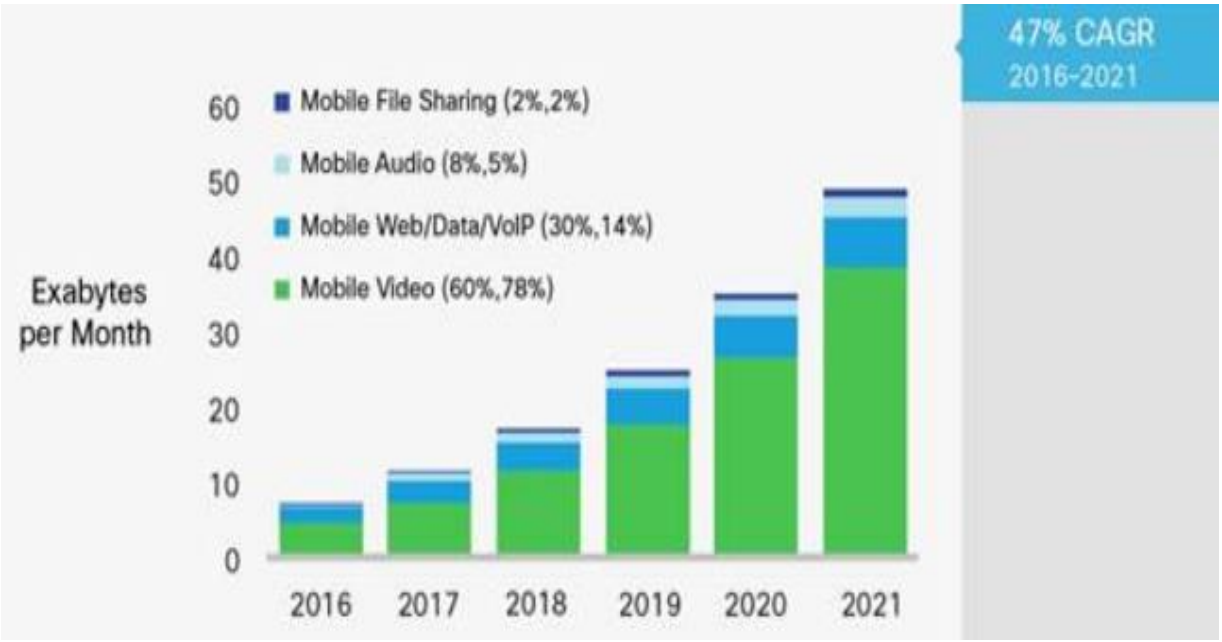

Figure 1. 4: The Mobile traffic share between (2016 and 2021) [7]

Figure (1.5) shows that the rapid decrease of the non-smart devices and connections from 54% percent at 2016 to 25% percent at 2021. While increasing of smart device and connections from 46% at 2016 to 75% at 2021.

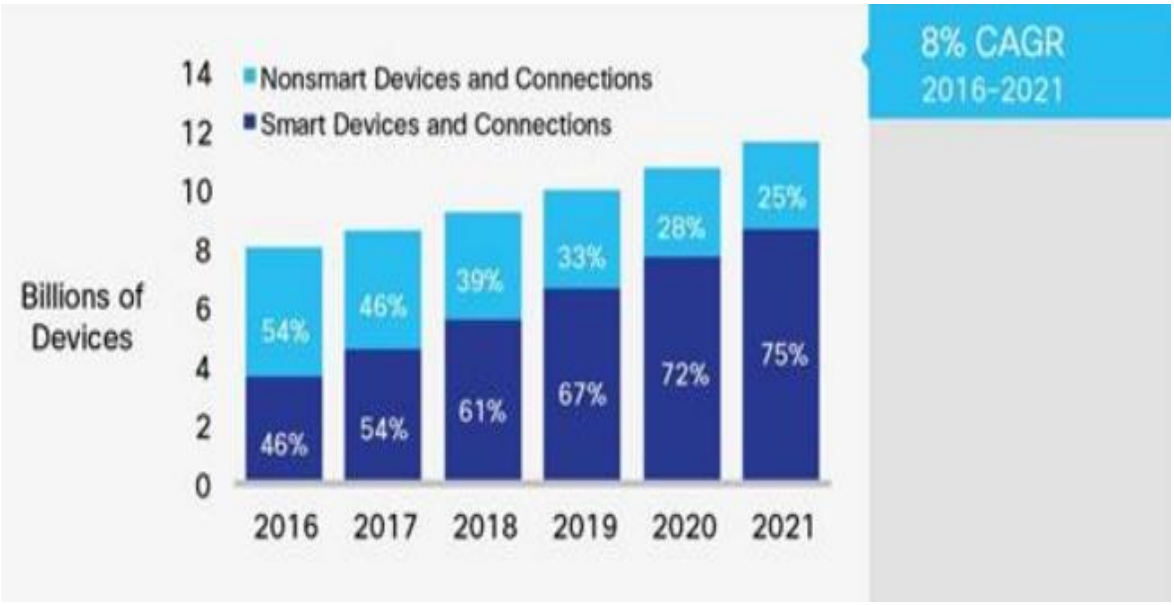

Figure 1. 5: Global Growth of smart devices and Connections between (2016-2021) [7]

Figure (1.6) displays the result of the growth of mobile smart devices and connections on global traffic. Globally, smart traffic is going to grow from 92%of the total global mobile traffic to 99% by 2021. This percentage is significantly higher than the ratio of smart devices and connections (75% by 2021) because on average a smart device generates much higher traffic than a non-smart device [7].

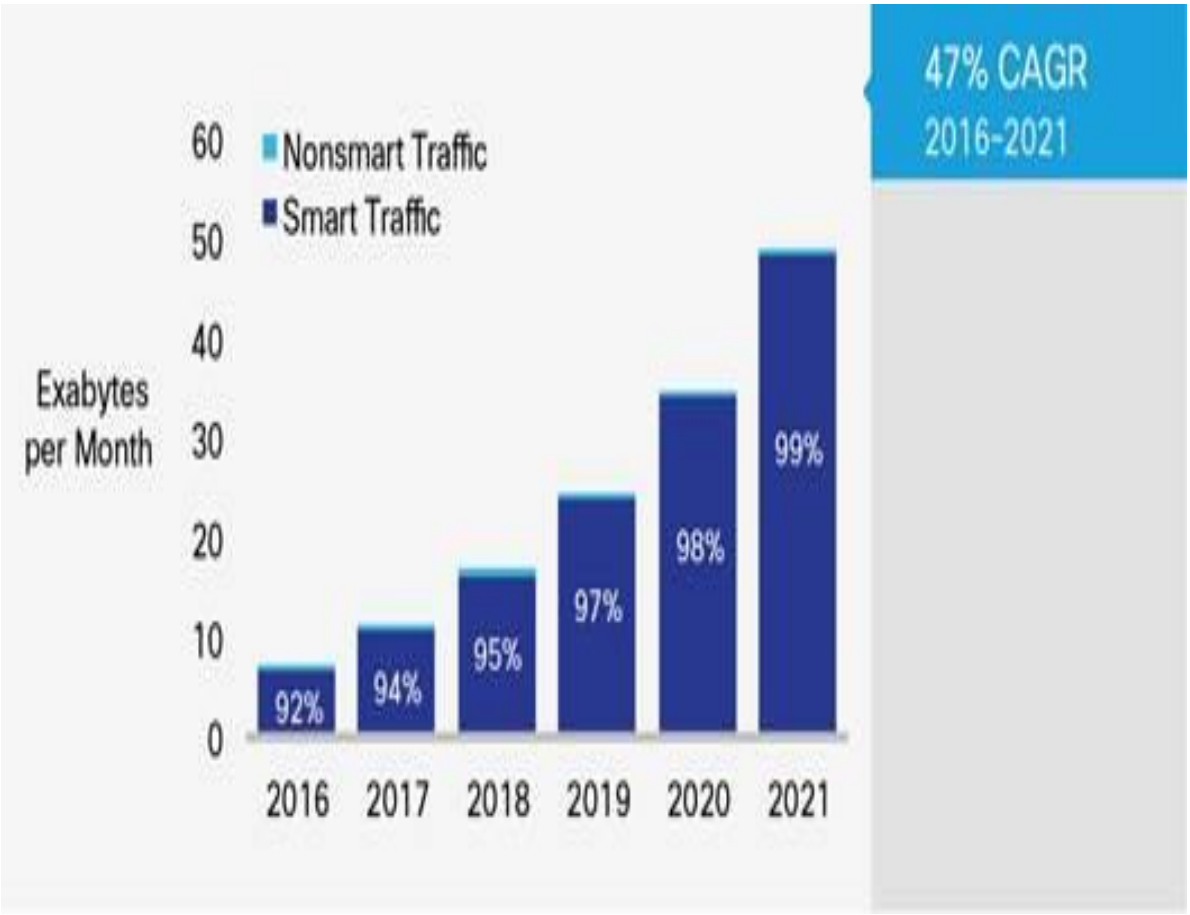

Figure 1. 6: Effect of Smart and non-smart mobile Devices and Connections Growth on Traffic [7]

1.3 **Multicarrier Modulation Systems (MCM)**

Wireless multicarrier communication systems technique is parallel data transmission where achieving high power spectral density (PSD) and data rates can be performed by the simultaneous transmission over multiple orthogonal subcarriers. Using MC communications, a wide-band frequency-selective fading channel is converted into many

narrow-band frequency non-selective flat fading sub-channels, facilitating channel estimation and equalization as well as time synchronization and narrowband interference mitigation [8]. In addition, the division of the whole bandwidth into many sub-channels provides scalability and flexibility when configuring the communication link and reducing inter-symbol interference (ISI). MCM has many advantages and disadvantages, the advantages of transmission data over Single carrier modulation (SCM) multicarrier are [9]:

1. Multicarrier modulation is baseband process that uses parallel equal bandwidth sub channels to transmit information. This leads to achieve higher spectral efficiency and high data rate.
2. Converting frequency selective fading channels into frequency flat fading by dividing the channel into narrowband flat fading subchannel. Moreover, it became easier to equalize at receiver.
3. Modulation can be for each subchannel if deep fading occur for this subchannel, then the power of this subchannel can compensate. Therefore, we can achieve power allocation.

The disadvantage of MCM are:

1. Higher sensitivity to the effect of narrow band noise, amplitude clipping, timing jitter and delay.
2. High peak to average ratio power ratio (PARP) associated with transmitted signal. High PARP cause in-band distortion and out of band emission (OOB). It also increases the complexity of analog to digital (A/D) and digital to analog converters and reduces the efficiency of radio frequency (RF) power amplifier used. Therefore, it is useful to reduce the PARP.

The following set of 5G is gaining industry acceptance [10]:

1. Support future applications like divers wide smart mobile, IoT, M2M, D2D, V2V.

2. Support higher data rates up to 10Gbps which is high 100 times 4G.
3. Support 10Tb/s per square kilometer which is 1000 times higher than 4G.
4. Support the increasing number of connected devices up to 1 million devices in square kilometer which is 1000 times higher than 4G. The total number of human-oriented terminals will be greater than 20 billion and the total number of IoT terminals will be greater than one trillion.
5. Latency less than 1ms which is lower 25 times than 4G
6. Support the fragmented spectrum to utilize the spectrum more efficiently.

1.3.1 Orthogonal Frequency Division Multiplexing multi-carrier (OFDM)

The most widely used multicarrier modulation technique is OFDM with CP. Due to the various advantages of OFDM, it has become the key physical layer transmission technology adopted in current broadband communication systems such as wireless local area networks (WLAN), worldwide interoperability for microwave access (WiMAX), long term evolution (LTE), ultra-wideband modulation (UWB) and digital video and audio broadcasting (DVB, DAB) [11, 12]. The OFDM system offers simple implementation using the inverse fast Fourier transforms (IFFT) and the fast Fourier transform (FFT) pairs in the modulator and demodulator [13,14]. respectively. However, the large side-lobes of the frequency response of the filters that characterize the subcarrier channels result in significant interference among subcarriers. The OFDM signal has a noise like amplitude with a very large dynamic range; hence it requires RF power amplifiers with a high peak to average power ratio [15,16]. It is more sensitive to carrier frequency offset and drift than single carrier systems are due to leakage of the DFT [17,18]. It is sensitive to Doppler shift. It requires linear transmitter circuitry, which suffers from poor power efficiency. It suffers loss of efficiency caused by cyclic prefix.

1.3.2 Filter Bank Multi-carrier (FBMC)

FBMC is short for filter bank multicarrier modulation technique. It is implemented based on IFFT/FFT pairs operation. It has numerous benefits over OFDM [8]. Firstly, it does not need cyclic prefix resulting in better use of the allocated spectrum. Secondly, instead of employing a rectangular window, a prototype filter implemented with the Nyquist pulse-shaping principle is adopted, which can minimize really the spectral leakage problem of OFDM. This results in negligible ISI and ICI. Thirdly, the grouping of filter banks with offset quadrature amplitude modulation (FBMC/OQAM), known also as OFDM/OQAM, leads to a maximum data transmission rate [8]. Fourthly, it is less sensitive to CFO by eliminate side lobes as the result of using digital filtering.

FBMC has many disadvantages. Firstly, the integration of MIMO with FBMC is very complex and as a result, limited systems have examined the use of these two techniques together. Secondly, the design of wide bandwidth and high dynamic range systems with FBMC provides some significant RF development challenges. Thirdly, FBMC is more complicated than OFDM; it introduces an overhead in overlapping symbols in the filter bank in the time domain.

1.3.3 Universal Filter Multi-carrier (UFMC)

Universal filtered multi-carrier (UFMC) modulation is a very powerful candidate to be employed for future 5G mobile systems. It overcomes the limitations and restrictions in current modulation techniques employed in 4G mobile systems such as orthogonal frequency division multiplexing (OFDM) and Filter bank multicarrier (FBMC). In addition, UFMC can support future applications like machine-to-machine (M2M), device-to-device (D2D), and vehicle-to-vehicle (V2V) communications. It is designed based on IFFT/FFT pairs

operation, Chebyshev window with Nyquist pulse-shaping principle is adopted, which can greatly reduce the spectral leakage problem of OFDM and FBMC [19-21].

1.4 **Literature review and contribution**

Fading channel estimation and equalizing techniques are crucial for coherent symbol detection at the receiver. Since the wireless channel is dynamically varying. The transmitted signal is sensitive to many effects during traveling to the receiver. The transmitted signal may be corrupted and the result is degradation of the performance of the wireless system. Transmitted signal travels in multipath and may be scattered or reflected, so the channel response varies according to the time. The statistical characteristics of the wireless communication system are environment dependent, Multipath fading, scattering, propagation, mobility cause the signal to spread in time, frequency and angle domains. All these affect the signal receiving. The channel estimation is very important to recover symbols.

Many techniques were used to estimate OFDM channel in the literature [22-27]. In addition, many techniques were employed to estimate FBMC channel [8][28-32]. On the other hand, there are limited researches on UFMC channel estimation [33-36]. Channel estimation techniques in the UFMC and FBMC/OQAM are different in traditional techniques used in OFDM due to the channel frequency response values are real in OFDM and complex in FBMC and UFMC. Another reason is the presence of intrinsic inter-symbol interference as the output of the filter. Due to subband filtering operation for out of band emission reduction may cause different filter gain at different subcarriers in one UFMC symbol [34]. Therefore, not all techniques used in OFDM is work for UFMC. For example, one of the techniques used in OFDM is polynomial interpolation not work probably due to different gain among pilot subcarriers and subcarriers. In [33], the authors show that conventional pilot-aided

channel estimation techniques used on CP-OFDM is work probably in UFMC by normalize filter gain for pilot subcarriers and make interpolation as in OFDM, then compensate filter gain again. In [34] the authors address the channel estimation and pilot signal optimization based on the comb-type pilot pattern based on least square linear interpolation, Discrete Fourier transform, Minimum mean square error, and relaxed minimum mean square error. The authors compares different techniques based on comb-type like a minimum mean square error (MMSE) that have higher complexity and knowledge of the channel correlation matrix and noise variance. Since the MMSE channel estimation require channel correlation matrix and noise power, other techniques are a relaxed minimum mean square error (RMMSE) that replaces the channel correlation matrix by power normalize identity matrix or diagonal matrix. While the least square with linear interpolation requires less complexity compared to MMSE and RMMSE. Discrete furrier estimator (DFT) has no interpolation error. In addition to the suggestion to use optimal pilot channel estimation by minimizing the minimum square error (MSE) to pilot power constraint and derive closed-form expression were derived. The simulation shows that MMSE has better performance than other techniques. Authors in [35] introduce using pseudo-random noise as the guard interval and the training sequence in the time domain to estimate the channel. Recently, the authors introduce estimation of UFMC time varying channel based on comb pilots using adaptive filters [36]. The fading channel process evolution is modelled by autoregressive model and track by Kalman filter. The result of simulation shows the performance of Kalman filter based estimator is better than LMS and RLS filters.

Using of combination of H_∞ estimator and autoregressive model to estimate UFMC system time varying channel not addressed to now. In this thesis, we will address estimation of fast flat time-varying fading Rayleigh channel in UFMC system. To exploit the characteristics of fading process linear time invariant. It is described by power spectral density (PSD) and

autocorrelation function (ACF). The fading channel will be modeled by autoregressive model (AR) system tracked by the H_∞ filter based on comb pilot technique. The AR parameters are calculated by Yule walker equation (YWE) based on zero order Bessel autocorrelation function.

The H_∞ filtering is more robust against the noise disturbances and modeling approximations than Kalman filtering]. It is principle is reducing the worst possible effects of the noise disturbances on the estimation error [23-27]. Moreover, this system does not need a priori constraints on the noises, except that they have limited energies. While Kalman filter is optimal in H_2 sense and required initial state, the driving process noise, and measurement noise are independent, white and Gaussian. Once the fading channel coefficients at pilot symbol positions are estimated by proposed techniques, the fading channel coefficients at data symbol positions are then estimated by using some interpolation techniques like linear, spline, or low pass interpolation.

The remainder of the thesis is formulated as follows. In chapter two, introduce the UFMC wireless system model where the transmitter, channel and receiver models are described clearly in addition to windowing function. In chapter three, we introduce fading channel estimation by explained pilot arrangement, Nyquist condition, Rayleigh fading channel, Autoregressive channel model, channel estimation and interpolation techniques. In chapter four, introduce a comparative simulation study is provided between the LMS, RLS, Kalman and H_∞ filters based channel estimators. Finally, conclusions, results and future work are presented in chapter 5.

Chapter 2

UFMC Wireless System Model

2.1 **Overview**

UFMC is a generalization of features of OFDM and FBMC and avoids their drawbacks. It is operation based on filter group of subcarriers called subbands. While OFDM operation filter for the whole spectrum. FBMC operation based on filter each subcarrier. UFMC structure implementation based on IFFT/FFT and Dolph Chebyshev filter. UFMC supports new application for 5G like M2M, D2D, and V2V, in addition, a large number of smart devices.

Section 2.2, we describe some of the window functions like a rectangular window, triangular window, raised cosine window, adjustable window and simulation comparison between Dolph Chebyshev with Hanning and Hamming windows. Transmitter, channel model and reciever of UFMC wireless system are presented in section 2.3. In Section 2.4, a comparison between UFMC, FBMC and OFDM systems will be carried out.

2.2 **Windowing Function**

We will introduce review of window functions. Since, the window functions used to minimize the leakage effects and for spectral analysis. The systems OFDM, FBMC and UFMC can use different window functions to reduce the spectral leakage. However, any

system can use different window functions. UFMC system can use window functions like Hamming, Hanning and Chebyshev windows…etc. Window technique is weighting function employed to data to decrease the spectral leakage correlated with finite observation periods. It is a mathematical function that is zero valued outside some chosen interval. The preferable window technique is the one that had minimum spectral leakage. [37-39] introduced survey in the literature about windows. Window techniques can be classified as fixed or adjustable [40, 41]. Fixed window refers to one independent parameter that controls the main lobe width by the length of the window. While the adjustable window refers to two or more independent parameters that control the window characteristics. In this type, the window length was fixed parameter and an additional one or more parameters control the window characteristics. We will introduce some of the types of windows functions:

2.2.1 Rectangular window

Rectangular window or zero canter is the simplest window. Its function based on replacing all by zeros except data sequence [39]. It is used in OFDM system. Its weight function expression as follows:

$$w_R(n) = \begin{cases} 1, -\frac{L-1}{2} \leq n \leq \frac{L-1}{2} \\ 0, \quad Otherwise \end{cases} \tag{2.1}$$

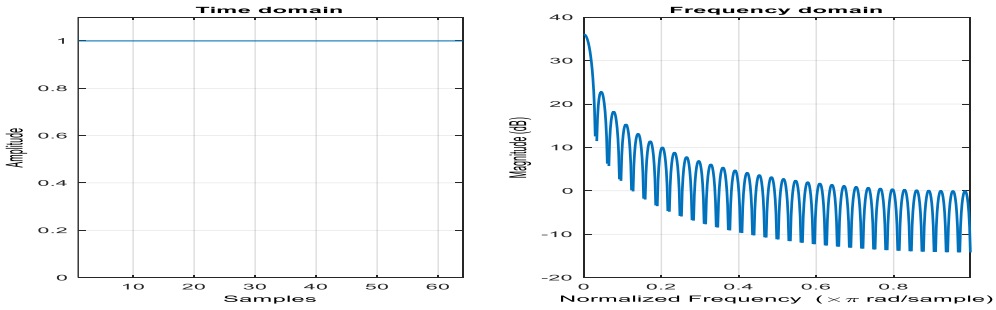

Figure 2. 1: Rectangular window in time and frequency domain for *L*= 64

Where L is the window length. The figure (2.1) shows the rectangular window in time and frequency domain for the window length $L = 64$.

2.2.2 Triangular window

It is known as Bartlett window or Fejer widow [39, 41]. It can be obtained by convolution of two $\frac{N}{2}$ width rectangular windows. It is weight function expression given by:

$$w(n) = 1 - \left| \frac{n - \frac{N-1}{2}}{\frac{L}{2}} \right| \text{, where } L \text{ can be } N, N+1, N-1 \qquad (2.2)$$

The figure (2.2) shows the triangular window for window length $L = 64$ in time and frequency domains.

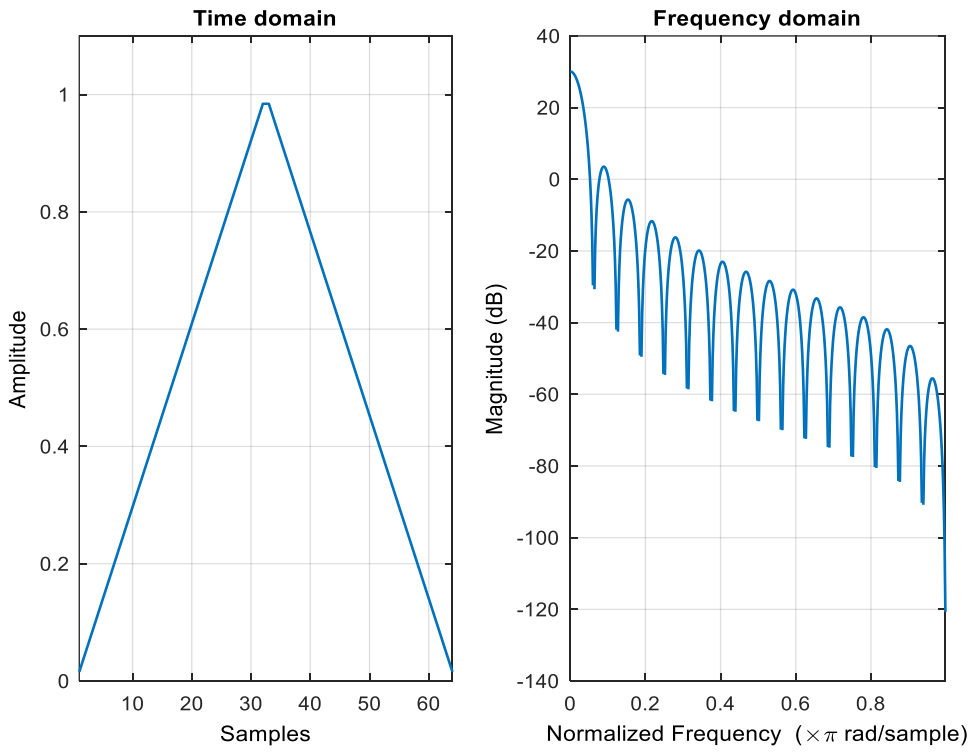

Figure 2. 2: Triangular window in time and frequency domain for L=64

2.2.3 Raised Cosine window

Raised Cosine window is another type of windowing that is smoother than triangular window at the ends and closer to the one at the middle [39,41]. Various kinds are:

2.2.3.1 Hanning Window

It is raised cosine weight function expressed as follow:

$$w_c(n) = \begin{cases} 0.5 - 0.5cos(\frac{2\pi n}{M} - 1), & 0 \leq n < M - 1 \\ 0, & Otherwise \end{cases} \quad (2.3)$$

The figure (2.3) shows the Hanning window in time and frequency domain for filter length $L = 64$.

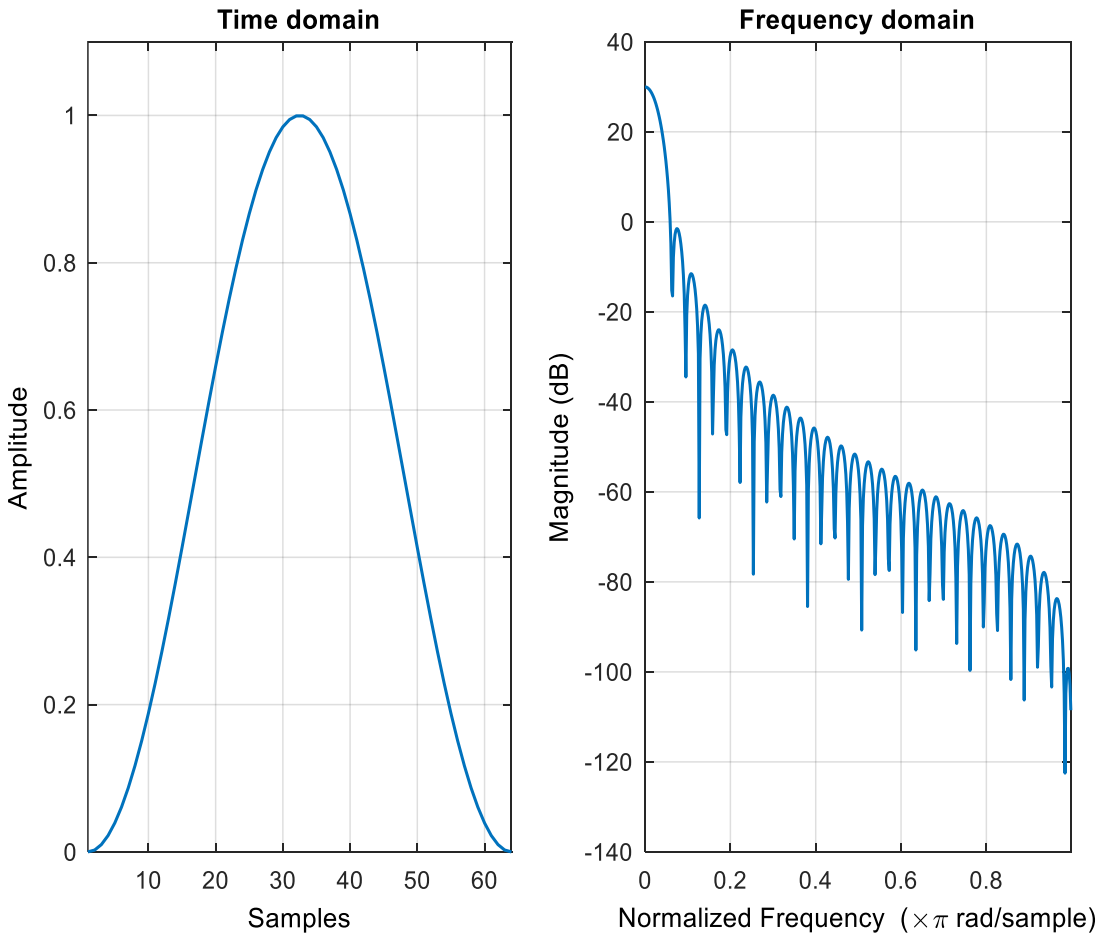

Figure 2. 3: Hanning window in time and frequency domain for L=64.

2.2.3.2 Hamming window

It is a weighting function defined by the following expression:

$$w_h(n) = \begin{cases} 0.54 - 0.46cos(\frac{2\pi n}{M} - 1), & 0 \le n < M - 1 \\ 0, & Otherwise \end{cases} \quad (2.4)$$

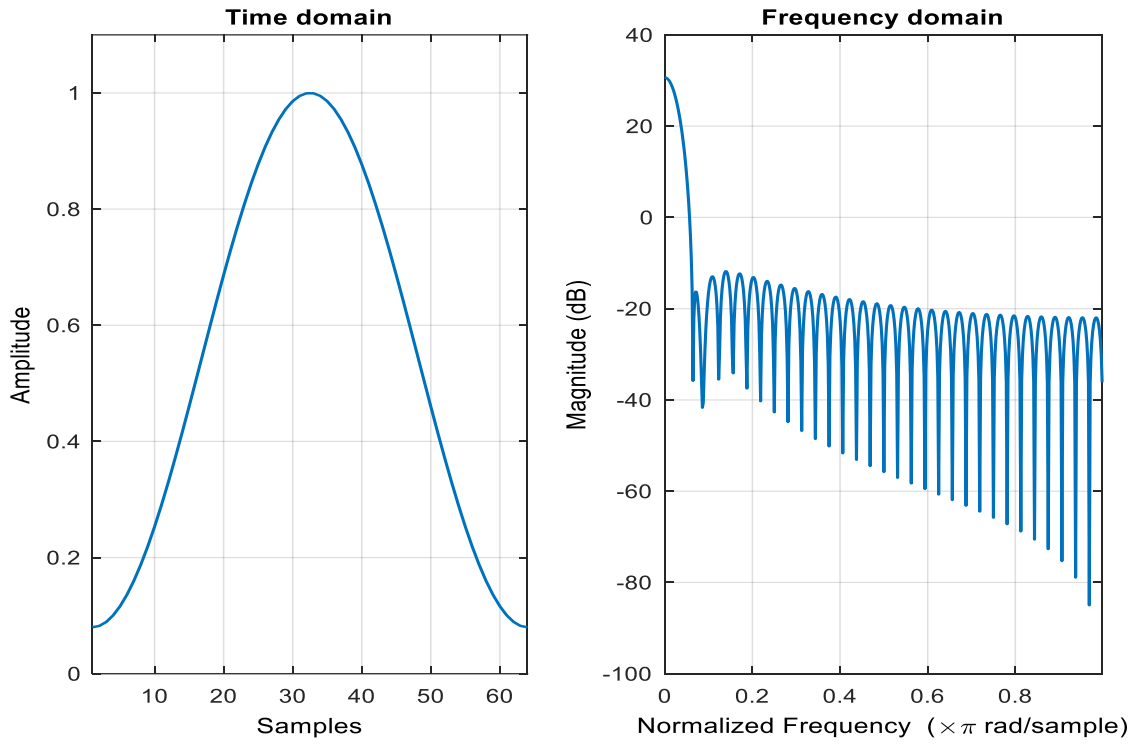

Figure 2. 4: Hanning window in time and frequency domain for L=64.

The figure (2.4) shows the Hamming window in time and frequency domain for window length $L = 64$.

2.2.4 Adjustable window

2.2.4.1 Gaussian Window

The Fourier transform of a Gaussian. Since the Gaussian function extends to infinity, it must either be truncated at the ends of the window or itself windowed with another zero-ended window. Since the log of a Gaussian produces a parabola, this can be used for nearly exact quadratic interpolation in frequency estimation:

$$w(n) = e^{-\frac{1}{2}\left(\frac{n-(N-1)/2}{\sigma(N-1)/2}\right)^2}, \sigma \leq 0.5 \quad (2.5)$$

The standard deviation of the Gaussian function is σ *(N−1)/2* sampling periods. Figure (2.5) shows Gaussian window in time and frequency domains for filter length $L = 64, \sigma = 3$.

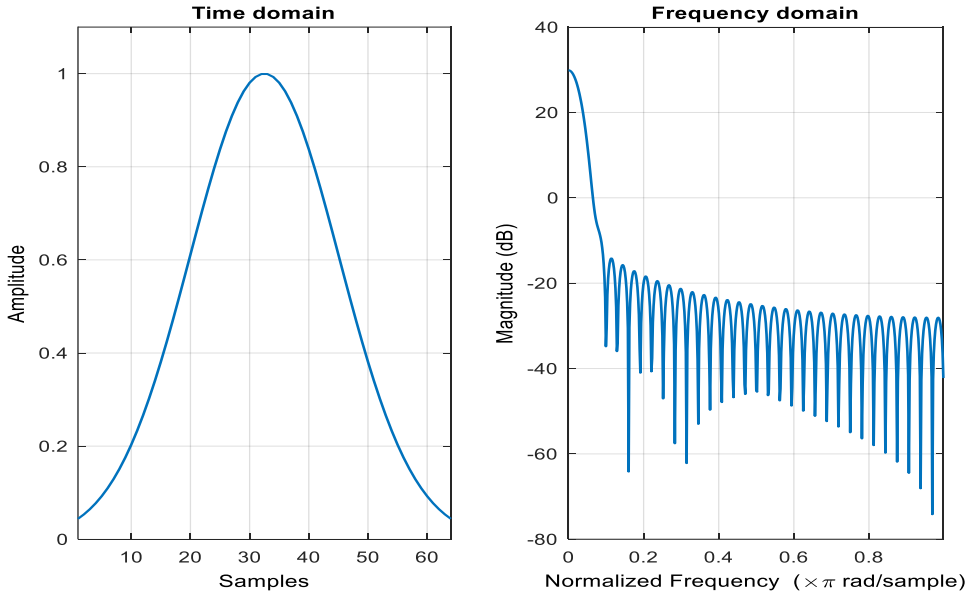

Figure 2. 5: Gaussian Window in Time and frequency domain for *L*=64.

2.2.4.2 Dolph Chebyshev Window

The Dolph-Chebyshev window filter is used in signal processing. One of the important properties is it has a minimum main-lobe width for a given side-lobe attenuation [37][39][42]. Furthermore, it has equi-ripple, which the side-lobe height is the same for all frequencies. The optimal Dolph-Chebyshev window transform can be given in the closed form by the following:

$$F(k) = \frac{cos\left\{Mcos^{-1}[\beta\, cos\left(\frac{\pi k}{M}\right)]\right\}}{cosh\{Mcosh^{-1}(\beta)\}} \quad (2.6)$$

Where:

$k = 0,1,2 \ldots M-1$ and M indicates IFFT Points , $\beta = cosh[\frac{1}{M}cosh^{-1}(10^{\alpha})]$, where α = (2, 3, 4).

The zero phase Dolph Chebyshev window $W_{0,k}$ is computed by IFFT of $F(k)$. The α parameters adjust the side lobe levels by the expression. Sidelobe level in dB=-20α. For example, if we have $\alpha = 3$ then the side lobes will be 60dB below the main lobe peak, where the main lobe peak normalize to zero. The chebyshev side lobes are called ripple in the stop band, since they are equal in heights. The mathematical expression for w_0 as the following:

$$w_0 = \frac{1}{N}\sum_{k=0}^{N-1} W_0(k).\, e^{\frac{i2\pi kn}{N}},\ \frac{-N}{2} \le n < \frac{N}{2} \qquad (2.7)$$

The characteristics of Dolph Chebyshev window in time and frequency domain. For given window length $L = 64$, $\alpha = 3$ where with side lobes 100dB below the main lobe peak as in figure (2.6).

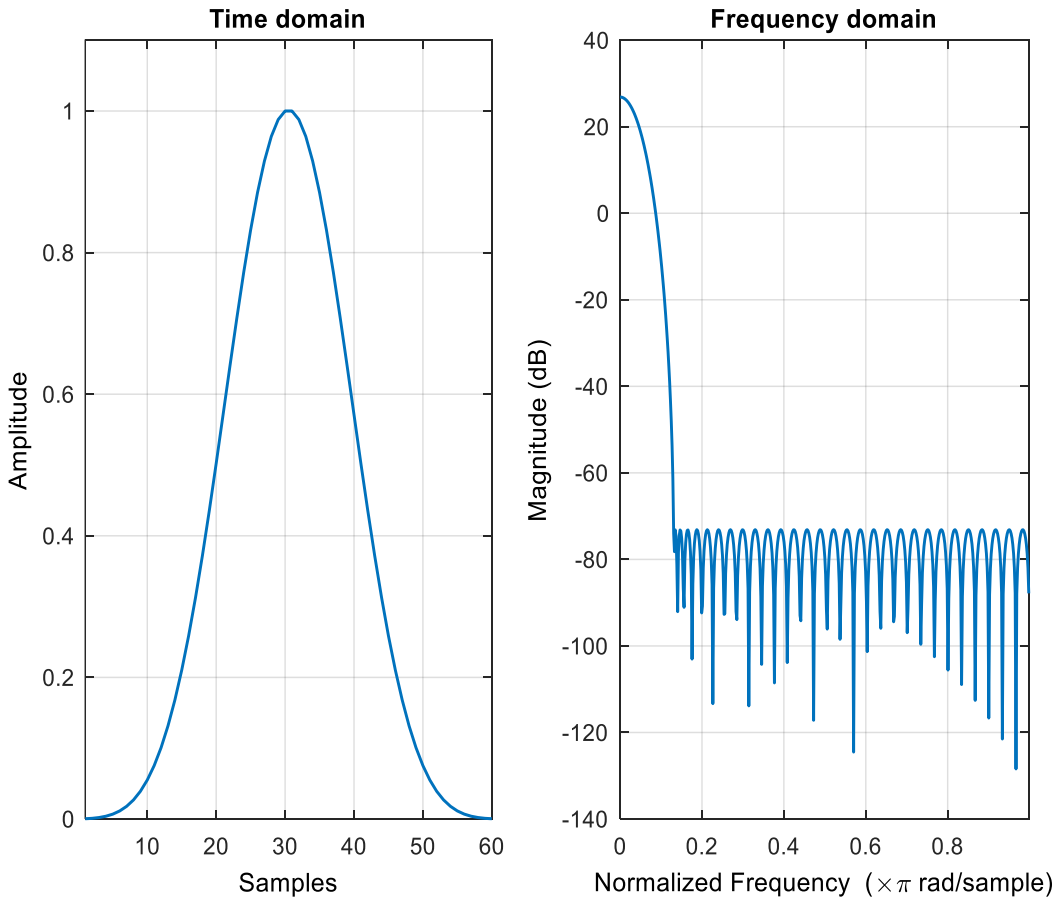

Figure 2. 6: Dolph Chebyshev window in time and frequency for L=64.

2.2.5 Dolph Chebyshev vs Hanning and Hamming

Simulation comparison in figure (2.7) between Dolph Chebyshev, Hanning and Hamming Windows.

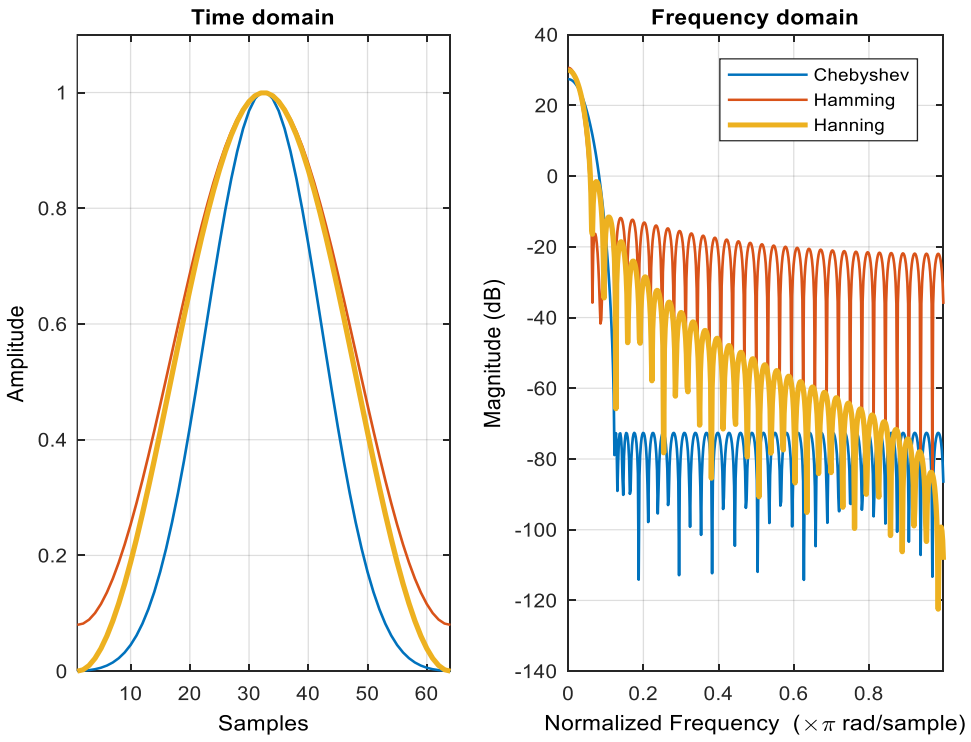

Figure 2. 7: Dolph Chebyshev window vs Hamming and Hanning.

For given window length $L = 64$. From the above figure, it can be observing that the response of Chebyshev window are more smooth and better than Hamming and Hanning windows. It has narrow side lobes width due to using extra cosine function and the result is increasing efficiency and less power lost. In the figure (2.8), the side lobes magnitude in chebyshev is about 100dB, while in Hamming and Hanning are 36dB, 22dB respectively. However, Chebyshev window have more computational complexity since it has many terms for calculation. Therefore, a compromise between the efficiency of window and computational complexity has to be found.

2.3 **UFMC Transceiver Model and Channel**

UFMC system with Chebyshev filters combine the advantages of OFDM and FBMC in addition to escaping their disadvantages. It filters group of subcarriers called subband. In addition, it still use QAM as it retains the complex orthogonality (when compared with FBMC), which works with existing MIMO schemes. UFMC system filters each subband in time, so spectrum range will be formed from conductive subbands as in figure (2.8) [43].

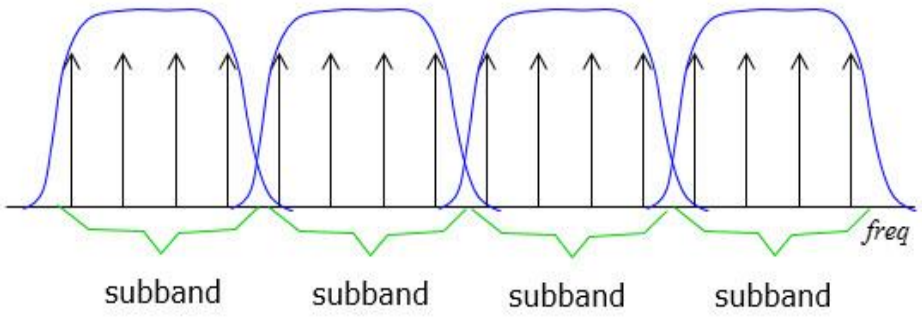

Figure 2. 8: UFMC signal in the frequency domain [43]

Table 2.1 shows comparative between three candidate modulation systems OFDM, FBMC and UFMC. It is clear that the UFMC system overcomes the other system in terms of overhead, short bursts, fragmented spectrum. The basic transceiver for UFMC is shown in figure (2.9).

Table 2. 1: Candidate system comparative.

	OFDM	**FBMC**	**UFMC**
PARP	High	High	High
Overhead	High	Low	Low
Receiver Complexity	Low	High	High
MIMO support	Yes	Yes	Yes
Short bursts	No	No	Yes
Fragmented Spectrum	No	Yes	Yes

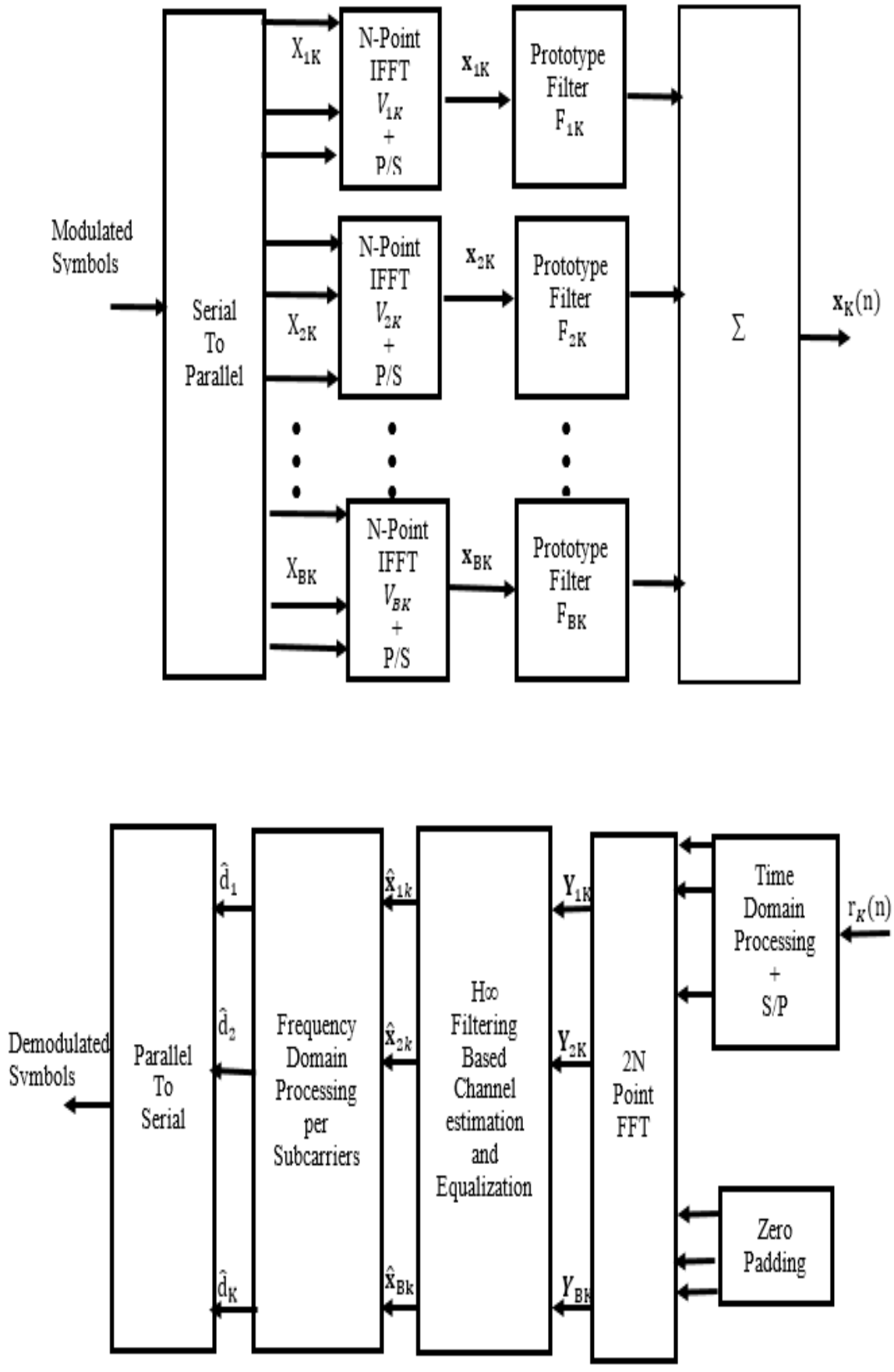

Figure 2. 9: UFMC Transceiver block diagram

2.3.1 UFMC Transmitter

The concept of the UFMC system is shown in figure (2.9) [35, 36]. The full band of subcarriers (*N*) is divided into subbands B. Each subband has a fixed number of subcarriers N_i^{Sub} and not all subbands need to be employed for a given transmission. An *N-pt* IFFT for each subband is computed, inserting zeros for the unallocated carriers. Each subband is filtered by Chebyshev filter $\mathbf{f} = [\mathrm{f}_0, \mathrm{f}_0, \ldots . \mathrm{L}_{\mathrm{f}-1}]$of length L_f and the responses from the different subbands are summed. The filtering is done to reduce the out-of-band spectral emissions (OOB). Different filters per subband can be applied, or the same filter is used for each subband. A Chebyshev window with parameterized side lobe attenuation is employed to filter the IFFT output per subband. We can express the discrete time UFMC data block base band signal in one symbol interval as follows [35-36]:

$$\boldsymbol{x}_k[n] = \frac{1}{N}\sum_{i=1}^{B}\sum_{l=0}^{N+L_f-1}\sum_{m=1}^{N_{Sub}^i} X_{iN}^m e^{j2\pi ml/N} f_{n-l} \qquad (2.8)$$

Where:

N: is the total number of subcarriers.

N_{Sub}^i: is the number of subcarriers in each subband

X_i^m: is transmission frequency domain data block

The number of subbands B will be different according application requirements. If the system used in the fragmented spectrum then *B* can be equal to the available spectrum portion in the fragmented spectrum. UFMC has the flexibility to filter each subband with its bandwidth. It is can enable the system to adapt users or service types by adjusting the subband and filter parameters only. UFMC can serve two different services like M2M and

tactile in two subbands with different requirements and frame structure without causing inter-symbol band interference (ISBI) due to lowering out of band emission [44].

2.3.2 Channel Model

The path between the base station and mobile stations of mobile communications is characterized by reflection, diffraction, and scattering of radio waves from objects such as buildings, hills, trees, etc. as shown in figure (2.10) [45]. As a result, the received signal consists of a superposition of several delayed and attenuated copies of the transmitted signal. This gives rise to frequency-selective fading which spreads the transmitted signal in time and, hence, leads to ISI. When all multi-paths arrive at the receiver within the symbol duration, the resulting fading is called frequency non- selective fading or flat fading. In addition to multi-path fading, due to the relative motion between the transmitter and the receiver and the movement of surrounding objects, the received signal is subject to Doppler shifts. This gives rise to time-varying fading. Hence, the transmitted signal through a mobile wireless channel may be generally affected by time-varying frequency-selective fading.

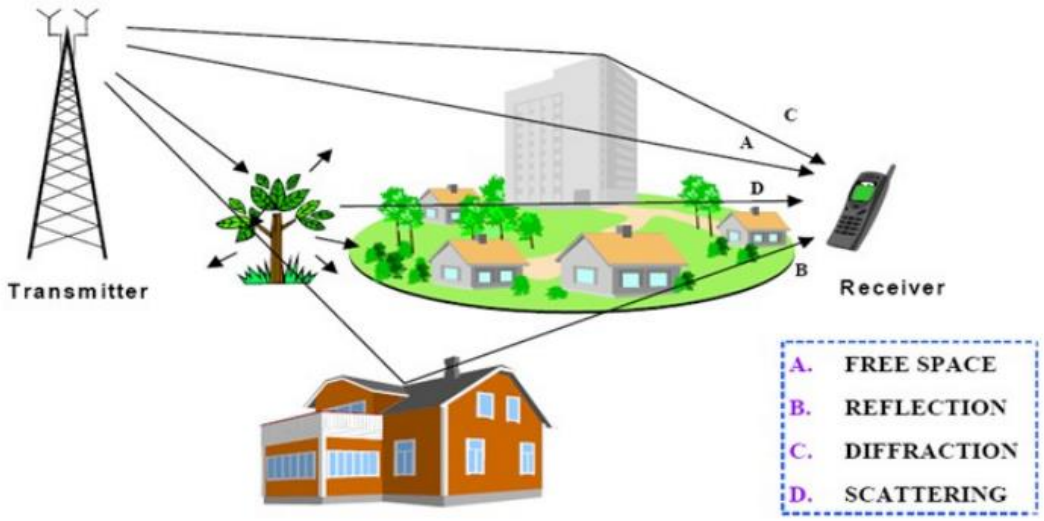

Figure 2. 10: Multipath fading channel [45]

The transmitted UFMC signal $x_k[n]$ in eq. (2.10) is assumed to go through a time-varying frequency-selective Rayleigh fading channel distribution $h_k[n]$ with background additive white Gaussian noise (AWGN) as shown in the Figure (2.11). Assuming that the allocated bandwidth for each subcarrier is less than the coherence bandwidth of the wireless channel, each subcarrier will undergo frequency non-selective flat-fading.

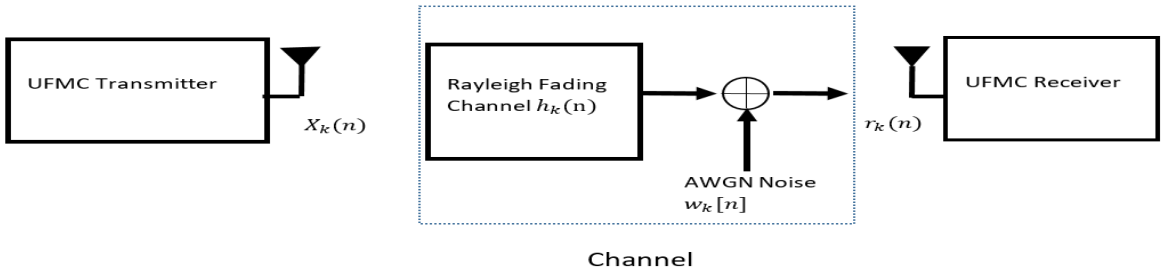

Figure 2. 11: Channel Model block diagram

According to Jakes [46], the frequency flat fading over n^{th} UFMC symbol can be modelled as the sum L_s scatters given as the sum of the weighted complex exponential:

$$h_k[n] = \sum_{l=1}^{L_s} g_{kl} e^{j(2\pi f_d n cos\varphi_{kl} + \vartheta_{kl})} \tag{2.9}$$

Where g_{kl}, φ_{kl} and ϑ_{kl}, are respectively the random scattered amplitude, angle of arrival and initial phase associated with l^{th} , k^{th} carrier, n^{th} UFMC symbol and f_d is Doppler frequency.

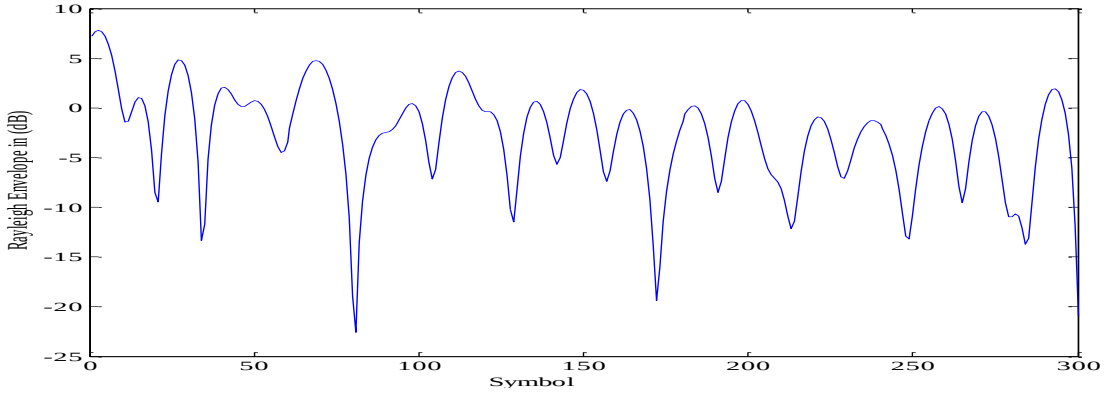

Figure 2. 12: Rayleigh envelope of $h_k(n)$ along the n^{th} UFMC symbol.

For a large number of multipaths, we can express approximation of $h_k[n]$ as Gaussian process $h_k[n] = |h_k[n]|e^{-j\varphi_k[n]}$. For case no line sight (NLOS) between transmitter and receiver, the fading process will have zero-mean. In that case, the phase $\varphi_k[n]$ is uniformly distributed on [0,2π] and the envelope $|h_k[n]| = h$ has the probability density function (pdf) as the following:

$$f_{\hbar}(h) = \begin{cases} \frac{\hbar}{\sigma_h^2} e^{-h^2/2\sigma_h^2}, & h \geq 0 \\ 0, & otherwise \end{cases} \quad (2.10)$$

Where $\sigma_h^2 = E[|h_k(n)|^2]$ is the variance of the fading process $\{h_k(n)\}_{k=0,1,\ldots,M-1}$. A typical Rayleigh distribution fading envelope and phase of time varying fading process $h_k(n)$ for $f_d T_s = 0.05$ are shown, respectively, in figure (2.12) and figure (2.13).

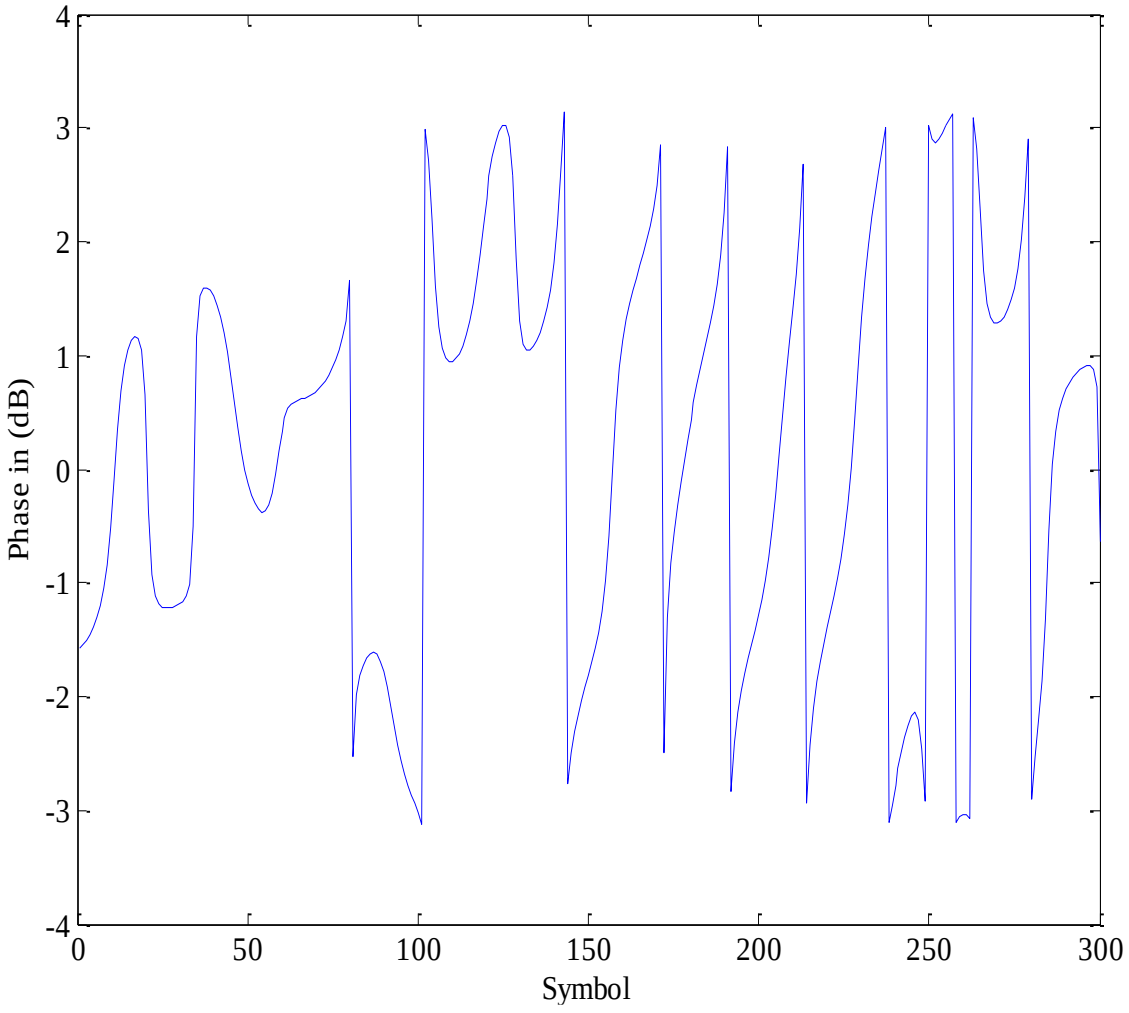

Figure 2. 13: Rayleigh phase of $h_k(n)$ along the n^{th} UFMC symbol.

For linear time invariant, the statistical properties for fading process $h_k[n]$ are given by power spectral density and autocorrelation function (ACF) as shown in the figure (2.14) and figure (2.15), respectively. The power spectral density PSD of $h_k[n]$ is defined by well-known U-shaped band limited Jakes spectrum with maximum Doppler frequency f_d:

$$S(f) = \begin{cases} \dfrac{1}{\pi f_d \sqrt{1-(f/f_d)^2}}, & |f| \le f_d \\ 0 \quad , & elsewhere \end{cases} \tag{2.11}$$

Where $f_d = \frac{v}{\lambda}$ with v is the mobile speed and λ is the wave length of the carrier wave.

The corresponding normalized discrete-symbols autocorrelation function (ACF) hence satisfies:

$$R_k = J_0(2\pi f_d T_s |k|) \tag{2.12}$$

Where $J_0(.)$ is the zero is order Bessel function of the first kind, T_s is the symbol period, and $f_d T_s$ is the Doppler rate.

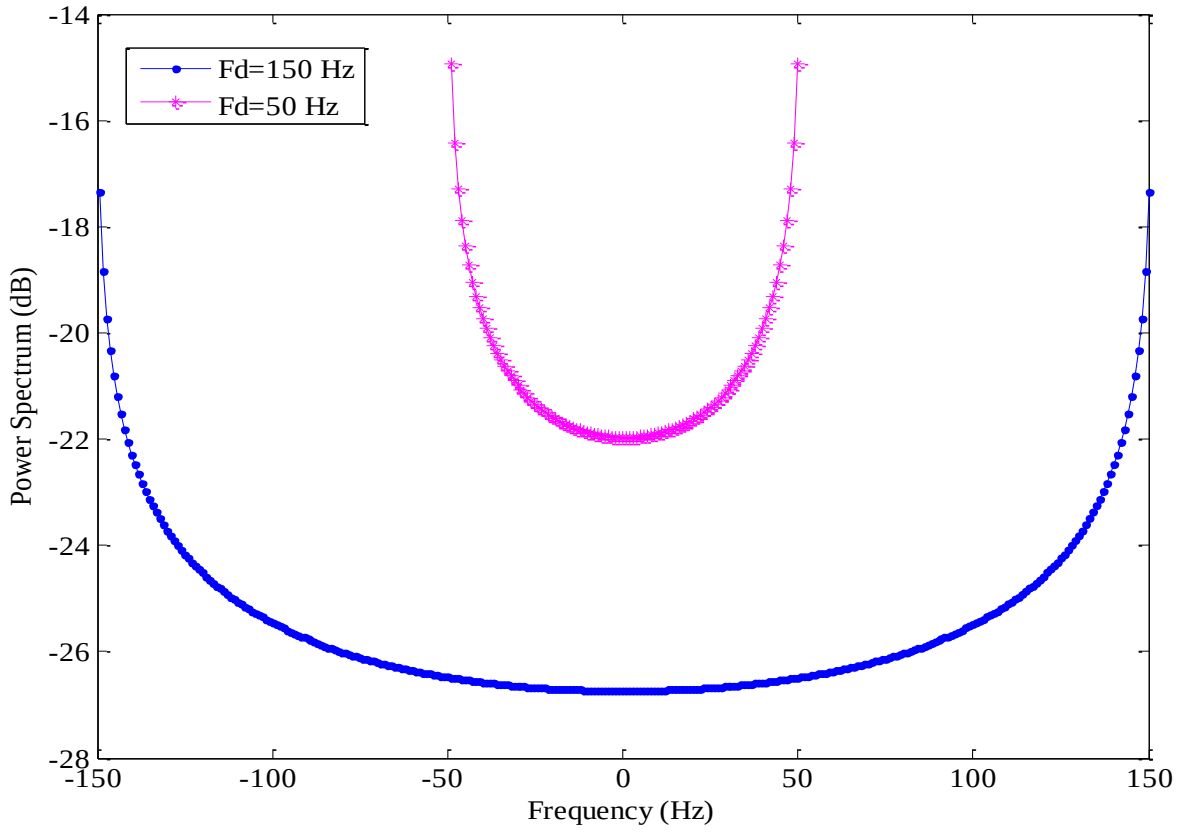

Figure 2. 14: PSD of $h_k(n)$ along n^{th} UFMC symbol

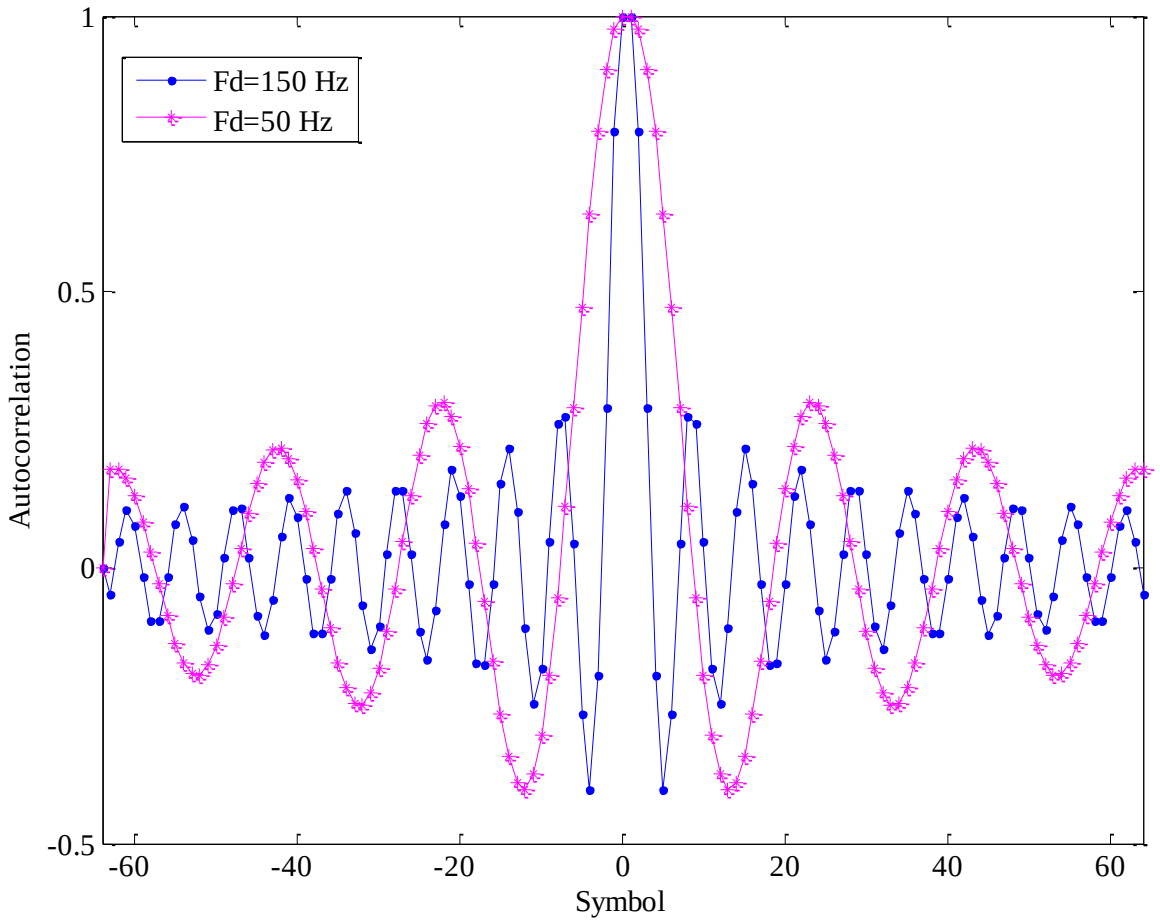

Figure 2. 15: Autocorrelation function of $h_k(n)$ along n^{th} UFMC symbol.

2.3.3 UFMC Receiver

The basic UFMC receive processing is the same OFDM system is based FFT. The received signal length $N + L_f - 1$ is then padded $N - L_f + 1$ to pass to the next $2N -$ FFT to convert it to frequency domain and to recover data symbols at N subcarriers from $N + L_f - 1$ received samples. Every alternate frequency value corresponds to a subcarrier main lobe. We assuming that the allocated bandwidth for each subcarrier is less than the coherence bandwidth of the wireless channel, each subcarrier will undergo frequency non-selective flat-fading. So, the received signal sample over the K^{th} subcarrier for n^{th} UFMC symbol as in the following :

$$r_k[n] = \boldsymbol{x}_k[n]\boldsymbol{h}_k[n] + w_k[n] \tag{2.13}$$

where $h_k(n)$ is a complex valued fading process over the k^{th} subcarrier for the n^{th} UFMC symbol, $w_k(n)$ is an additive white Gaussian noise (AWGN) process. The noise processes $\{w_k(n)\}_{k=0,1,\ldots,M-1}$ are assumed mutually independent and identically distributed zero-mean complex Gaussian processes with equal variances σ_w^2. The output of FFT will be converted to serial again then symbol demapper retrieve original data.

2.4 **UFMC vs OFDM and FBMC**

The figures (2.16- 2.18) shows that the power spectral density for UFMC, OFDM and FBMC systems respectively for the same number of subcarriers (200).

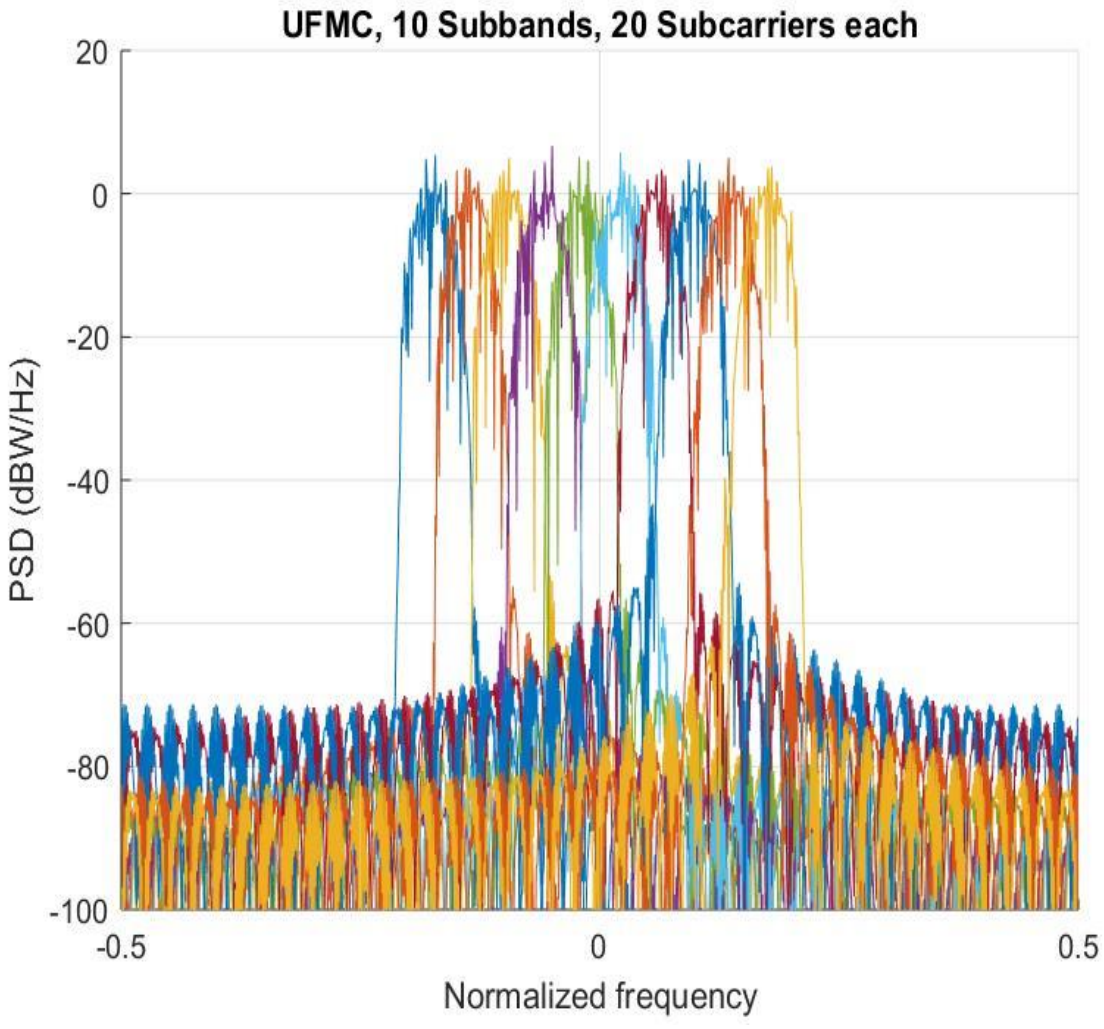

Figure 2. 16: Power Spectral Density for UFMC System

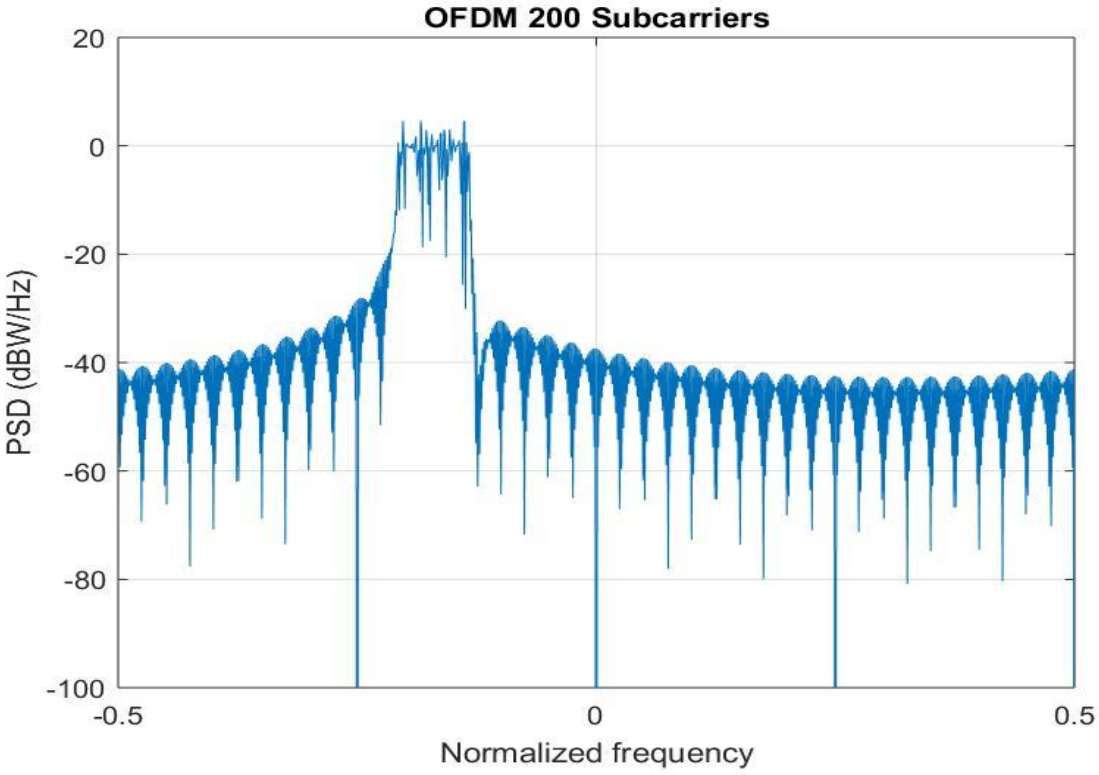

Figure 2. 17: Power Spectral Density for OFDM System

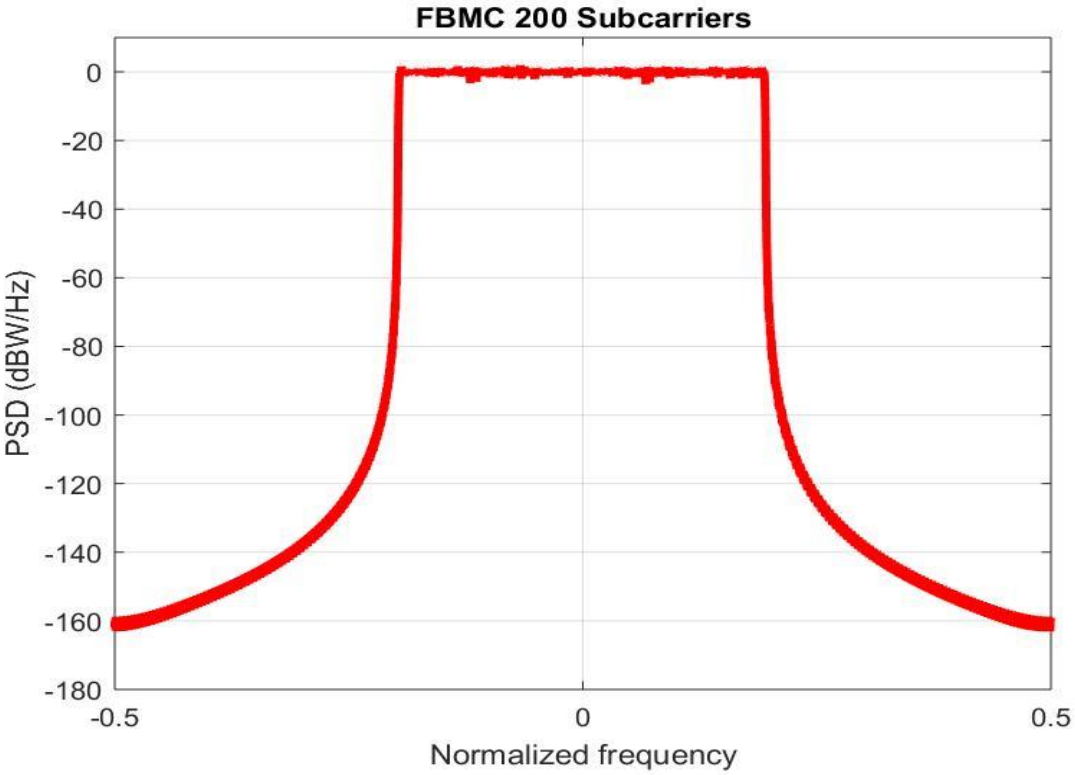

Figure 2. 18: Power Spectral Density for FBMC System

From above figures, it is clear that UFMC is the best system comparison to OFDM and FBMC by offering higher spectral efficiency (PSD) due to minimizing side lobes. Subband filtering has the benefit of reducing the guards between subbands and reducing the filter length, which makes this system attractive for short bursts comparison to FBMC that required longer filter length, which make it not supported short burst application.

Chapter 3

Fading Channel Estimation and Equalizing

3.1 State of the art

Many channel estimation techniques were proposed in the literature particularly for OFDM systems [22-27]. They can be divided into training sequence/pilot symbols based techniques and blind techniques [47-48]. The blind techniques require no training data. They utilize certain underlying mathematical information about the kind of data being transmitted. As blind techniques require a large amount of data, they are extremely computationally intensive and hence are impractical for real-system implementation [47]. For this reason, we will focus our attention on the training sequence techniques in this thesis. The training sequence/pilot symbols based techniques are used in some existing mobile and wireless communication systems. The idea of training sequence/pilot symbols based techniques is that some portion of the transmitted signal is known to the receiver and used for channel estimation. Many techniques were introduced in literature to estimate FBMC channel [8][28-32].

Compared to OFDM and FBMC, the literature on UFMC that addressed the problem of channel estimation and equalization are limited [33-36]. In the FBMC/OQAM and UFMC approach, the channel estimation issue is different of that in conventional techniques in

OFDM. The reason is that, the sought channel frequency response values are complex whereas the training input is real. Another reason is the presence of intrinsic inter-symbol interference as the output of the filter. In addition, due to subband filtering operation for out of band emission reduction may cause different filter gain at different subcarriers in one UFMC symbol [34]. So, not all techniques in estimation OFDM system can be used in FBMC and UFMC systems.

In [33], the authors investigate the procedure and performance of sliding window and linear interpolation techniques in UFMC system in an uplink multi-user FDMA scenario in presence of cyclic prefix. Authors show that the classical channel estimation and equalizing methods are applicable at the receiver in UFMC as in OFDM. In [34], the authors proposed channel estimation schemes and pilot signal optimization for UFMC system based on the comb pilot pattern. By considering the least square linear interpolation (LSLI), discrete Fourier transform (DFT), minimum mean square error (MMSE) and relaxed MMSE (RMMSE) channel estimators. In [35], authors introduce using pseudo-random noise as the guard interval and the training sequence in the time domain to estimate the channel. In [36], authors present estimation of UFMC time varying channel based on comb pilots using adaptive filters based estimators. The fading channel process evolution is modelled by autoregressive model and track by Kalman filter. The result of simulation shows the performance of Kalman filter based estimator is better than LMS and RLS filters.

3.2 **Pilot pattern**

There are different types of pilot's arrangement that are used in UFMC channel estimation. The most famous types are block, comb and rectangular pilot patterns.

3.2.1 Block type pilot Arrangement

In block pilot pattern illustrated by figure (3.1), UFMC channel estimation symbols are transmitted periodically, in which all subcarriers are used as pilots [49]. The typical channel estimation methods for block pilot pattern are LS and MMSE. This type is suitable for frequency selective fading channel.

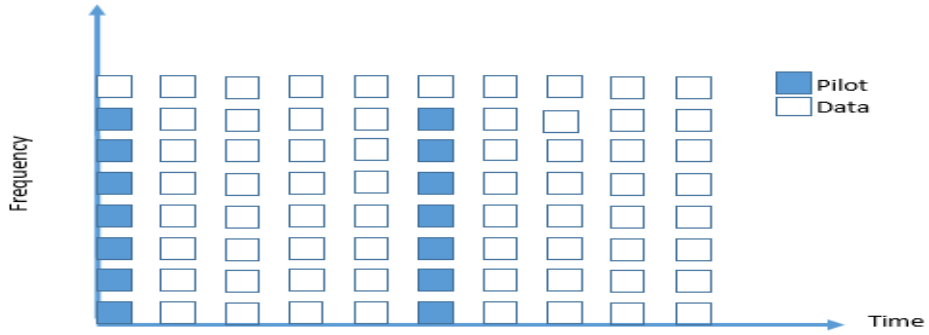

Figure 3. 1: Block type pilot arrangement

3.2.2 Rectangular Pilot Arrangement

Rectangular pilot pattern where UFMC blocks with comb pilots are sent periodically in a non-continuous manner. In this thesis, we focus our attention on the comb pilot patter.

3.2.3 Comb Pilot Arrangement

In comb pilot pattern illustrated by figure (3.2), some of the subcarriers are reserved for pilots for each symbol. Comb pilots are suitable for a fast fading channel but not for frequency selective channels. The typical channel estimation methods for block pilot pattern are LS and MMSE. Channel interpolation in digital signal processing (DSP) points to the method of transform a sampled digital signal such as a sampled audio signal to that of a higher sampling rate. Channel interpolation compatible with comb pilot techniques are linear

interpolation (LI), low-pass interpolation (LPI), second order interpolation (SOI), spline cubic interpolation (SCI) [50-51].

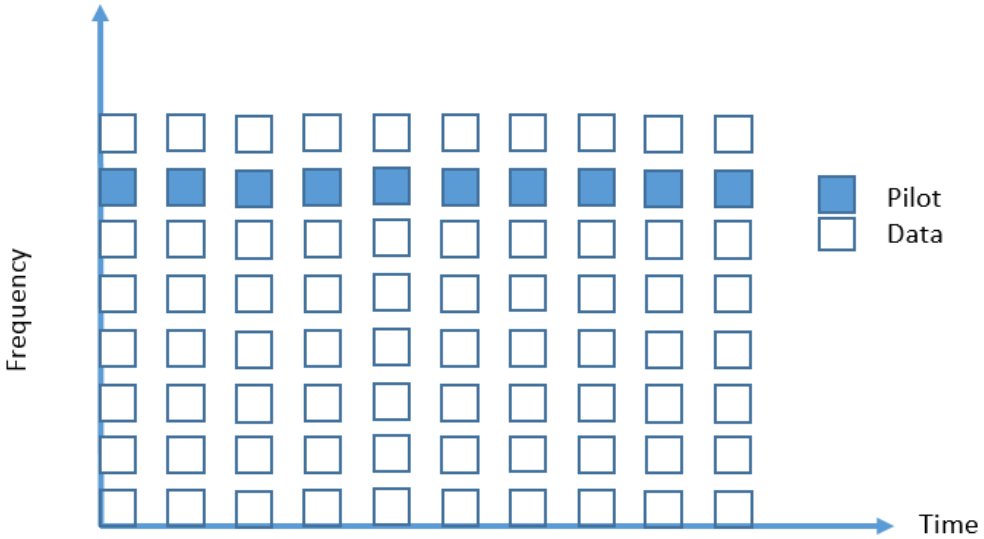

Figure 3. 2: Comb type Pilot Arrangement

In this thesis, we focus our attention on the channel estimation using comb pilot arrangement.

3.3 **Nyquist Condition**

In wireless communication systems, the Nyquist condition is essential to ensure the accurate rebuilding of the transmitted signals. Perfectly, the filter pulse response $h(n)$ is assumed to satisfy the next equation in the time domain:

$$g(n) = \begin{cases} 1, & n = L-1 \\ 0, & n = kM, n \neq L-1 \\ arbitrary, & n \neq kM \end{cases} \quad (3.1)$$

Or equivalent to power -complementary property in frequency-domain, which could be express by the following expression [52-53]:

$$\sum_{k=0}^{M-1} \left| G\left(e^{j(w+\frac{2\pi}{M}k)}\right| = 1, w \in \left[0, \frac{\pi}{M}\right] \right. \quad (3.2)$$

For above Nyquist conditions, M indicate an integer named over-sampling factor. Moreover, $g(n)$ expresses the parameters of the Nyquist filter. Usually, condition (1) and (2) are too restrictive for square root -Nyquist filter, since the Nyquist condition can be release for the enhancement of other filter performances such as the frequency selectivity of the filter. Even though, the deviation of the Nyquist condition might present interference between consecutive samples, it is commonly small when compared to the residual interferences due to the propagating channel. The designed filters with the sacrificed Nyquist condition had been successfully used in FBMC for better robustness [54].

3.4 **Autoregressive (AR) Channel Modeling**

One of the features of the MCM system is converting selective fading channel to flat fading channel. Sum of sinusoids (SOS) based simulator or on the inverse discrete Fourier transform (IDFT) based simulator were proposed to generate correlated Rayleigh random variables [55-58]. The advantage of SOS is generation accuracy very long sequence without impact on computer memory. However, the fading process not wide sense stationary (WSS) [59]. IDFT based simulator is relatively very fast and able to generate sequence corresponding to given ACF. Its applicability is limited due to large memory space requirement. To generate accurately correlated Rayleigh processes that shape the spectrum of the uncorrelated Gaussian variates, the authors proposed to use general AR model [60]. It is different from another model that is there is an accurate matching of theoretical statists over an order of model and it is simple and linear. The fading process is modeled as a complex Gaussian process, where the variability of the channel over time is presented by ACF. The statistical properties of linear time invariant fading channel are described by its PSD and ACF in eq. (2.18, 2.19) in chapter 2 respectively.

The complex fading process can be modeled by a p^{th} AR (p) in [60] and defined as the following expression:

$$\boldsymbol{h}_k(n) = -\sum_{i=1}^{p} a_i \boldsymbol{h}_{k-i}(n) + \boldsymbol{v}_k(n) \tag{3.3}$$

Where $v_k(n)$ is denoted for complex white Gaussian noise process with uncorrelated real and imaginary elements with driving process ${\sigma_v}^2$. $\{a_i\}_{i=1,2,\ldots,p}$ denote to the AR parameters. The PSD of the AR(p) model can be expressed by [61] as follows:

$$S(f_n) = \frac{\sigma_v^2}{\left|1 + \sum_{i=1}^{p} a_i e^{(-j2\pi f_n i)}\right|^2} \tag{3.4}$$

Where f_n denote to the normalized frequency.

The relation between AR parameters and the fading process autocorrelation function can be express by Yule-Walker equation (YWE) [61] as the following:

$$\boldsymbol{R\theta} = -\boldsymbol{r} \tag{3.5}$$

where $\boldsymbol{R}$ is the fading channel autocorrelation matrix defined by:

$$\boldsymbol{R} = \begin{bmatrix} R_0 & R_{-1} & \cdots & R_{-p+1} \\ R_1 & R_0 & \cdots & R_{-p+2} \\ \vdots & \vdots & \ddots & \vdots \\ R_{p-1} & R_{p-2} & \cdots & R_0 \end{bmatrix} \tag{3.6}$$

$\boldsymbol{\theta}$ is the vector that contains the AR parameters as follows:

$$\boldsymbol{\theta} = \begin{bmatrix} a_1 \\ a_2 \\ \vdots \\ a_p \end{bmatrix} \tag{3.7}$$

and

$$\boldsymbol{r} = \begin{bmatrix} R_1 \\ R_2 \\ \vdots \\ R_p \end{bmatrix} \tag{3.8}$$

The variance of driving process σ_v^2 can be expressed as:

$$\sigma_v^2 = R_0 + \sum_{i=1}^{p} a_i R_{(-i)} \tag{3.9}$$

Increasing the AR mode order p will provide better fitting between the resulting model and the theoretical PSD and ACF [60]. Baddour et al [60] use high order AR process (e.g. $p \geq 50$) when they simulated the channel. For this purpose, they modify the properties of the channel by considering the sum of the theoretical fading process and zero-mean white process whose variance very small. Then, the AR parameters are estimated with the YWE based on the modified autocorrelation function:

$$R_k^{mod} == J_0(2\pi f_d T_s |k|) + \varepsilon\delta_k \tag{3.10}$$

where ε is a very small bias used to overcome the ill conditioning of YWE .

However, the computational complexity of the resulting channel estimation algorithm will also increase. Therefore, a compromise between the accuracy of the model and the computational complexity of the estimation algorithm has to be found. AR order must be determined. Taking into account a higher AR model order will be more accurate. But higher AR model order will be more computational. Therefore, a compromise between the channel estimation accuracy and computational complexity has to be found. To simplify the process and lower computational cost we select the AR process $p = 2$. Then the AR parameters will have calculated by Yule-walker equations (YWE) based on the autocorrelation function (ACF).

3.5 **Channel estimation**

The estimation of the fading process $h_k(n)$ along the n^{th} UFMC symbol will be performed in two steps. Firstly, the fading process $h_k(n)$ at the pilot symbol position is estimated using LMS, RLS, Kalman filters and H_∞ filter. Secondly, the fading process at data symbol

position will then be estimated by using some interpolation methods such as linear, spline or low-pass interpolation.

When using a comb-type pilot arrangement [62] as shown in Figure 3.2, N_p pilots are uniformly inserted into $x_k(n)$ as follows:

$$\boldsymbol{x}_k(n) = x_{uL+i}(n) = \begin{cases} x_{uL,pilot}(n), & i = 0 \\ x_{uL+i,data}(n), & i = 1,2 \cdots, L-1 \end{cases} \quad (3.11)$$

Where $x_{uL,pilot}(n)$ is the u^{th} pilot symbol with the $u = 0,1, \ldots, N_p - 1$, and $L = M/N_p$ is the pilot interval spacing with M the number of subcarriers.

3.5.1 Fading process estimation at pilot symbol positions

The basic technique for comb-pilot estimation is based on the least square error (LS) and minimum mean square error (MMSE). The estimation process is divided into two stages. The first stage of estimation is estimation the fading process $h(n)$ over the n^{th} UFMC symbol based on adaptive filters (LMS, RLS, Kalman and H_∞ filters). Note that, for the sake of simplicity and clarity of presentation, the time index subscript is dropped. Thus, the fading process $h(n)$ is reduced to $h_k(n)$. The second stage is to estimate symbols based on interpolation techniques.

3.5.1.1 Least Mean Square (LMS) filter

LMS adaptive filter is one of the suggested filters to estimate the impulse response channel $\hat{h}(n)$ of the fading channel $h(n)$ and make it closely as possible to $h(n)$ by minimizing the Mean Square Error (MSE) as follows:

$$MSE = E[|x(n) - h(n)r(n)|^2] \quad (3.12)$$

The channel estimates at tap $k + 1$ is given by:

$$\hat{h}(n+1) = \hat{h}(n) + \mu\big(x(n) - \hat{h}(n)r(n)\big)r^*(n) \tag{3.13}$$

$$\hat{h}(n+1) = \hat{h}(n) + \mu e(n)r^*(n) \tag{3.14}$$

Where μ the LMS is step size which can be adjusted manually by the designer or automatically to realize the best performance requirements. x_k denote for the transmitted signal. r_k is the expression for the received signal. While p denote for filter order. The initial parameters are:

$$\hat{h_0} = zeros(p)$$

3.5.1.2 Recursive Least Square (RLS) Filter

RLS adaptive filter is another suggested adaptive filter to estimate impulse channel response $\hat{h}(n)$ of the fading channel h(n) based on minimizing the weight LS cost function as follows:

$$F = \sum_{i=0}^{k} \lambda^{k-1} |x(n) - h(n)r(n)|^2 \tag{3.15}$$

Where:

λ denote for the forgetting factor and has a value$0 < \lambda < 1$.

The channel estimates at $k+1$ is given by:

$$\hat{h}(n+1) = \hat{h}(n) + \big(x(n) - \hat{h}(n)r(n)\big)\boldsymbol{K}^*(n) \tag{3.16}$$

$$K(n) = \frac{P(n)r(n)}{\boldsymbol{\lambda} + P(n)r(n)r^*(n)} \tag{3.17}$$

$$P(n+1) = \lambda^{-1}\big(1 - K(n)r^*(n)\big)P(n) \tag{3.18}$$

Where $K(n)$ is the so-called Kalman gain. The initial parameters assumption as follows:

p denote for filter order.

$\boldsymbol{P}_0 = \mathbf{I}$: Identity matrix of rank $p+1$

3.5.1.3 Kalman Filters

Another suggested filter to estimate channel impulse response $\hat{h}_k$ of the fading process $h_k(n)$ is Kalman filter .

To estimate the fading process $h_k(n)$ over the n^{th} UFMC symbol based on Kalman filtering with known pilot symbols. To this end, let us define the state vector as follows:

$$\boldsymbol{h}(n) = [\, h(n) \;\; h(n) \;\; \ldots h(n-p+1) \;\;]^T \tag{3.19}$$

Then, equation (3.18) can be written in the following state-space form:

$$\boldsymbol{h}(n) = \boldsymbol{\phi}\boldsymbol{h}(n-1) + \boldsymbol{g}v(n) \tag{3.20}$$

Where:

$$\boldsymbol{\phi} = \begin{bmatrix} -a_1 & -a_2 & \cdots & -a_p \\ 1 & 0 & \cdots & 0 \\ \vdots & \vdots & \ddots & \vdots \\ 0 & \cdots & 1 & 0 \end{bmatrix} \text{ is the transition matrix and } \quad \boldsymbol{g} = [1\ 0\ \ldots 0]^T \tag{3.21}$$

In addition, given equations (3.15) and (2.20), it follows that:

$$r(n) = \boldsymbol{x}^T(n)\boldsymbol{h}(n) + w(n) \tag{3.22}$$

Where $\boldsymbol{x}(n) = [\, x_{pilot}(n) \;\; 0 \;\cdots\; 0]^T$

Hence, equations (3.33) and (3.17) represent the state-space model dedicated to the n^{th} UFMC symbol fading channel system (3.22) and (3.24). A standard Kalman filtering can be carried out to provide the estimation $\widehat{\boldsymbol{h}}(n/n)$ of the state vector $\boldsymbol{h}(n)$ given the set of observations $\{r_i\}_{i=1,\cdots,K}$. To this end, let us introduce the so-called innovation process $\alpha(n)$ which can be obtained as follows:

$$\alpha(n) = r(n) - \boldsymbol{x}^T(n)\boldsymbol{\phi}\widehat{\boldsymbol{h}}(n-1/n-1) \tag{3.23}$$

The variance of the innovation process can be expressed as:

$$C(n) = E[\alpha(n)\alpha^*(n)] = \boldsymbol{x}^T(n)\boldsymbol{P}(n/n-1)\boldsymbol{x}(n) + \sigma_w^2 \tag{3.24}$$

Where the so-called *a priori* error covariance matrix $\mathbf{P}(\mathrm{n}/\mathrm{n}-1)$can be recursively obtained as follows:

$$\boldsymbol{P}(n/n-1)=\boldsymbol{\phi}\boldsymbol{P}(n-1/n-1)\boldsymbol{\phi}^{H}+\boldsymbol{g}{\sigma_{\upsilon}}^{2}\boldsymbol{g}^{T} \tag{3.25}$$

The Kalman gain is calculated in the following manner:

$$\boldsymbol{K}(n)=\boldsymbol{P}(n/n-1)\boldsymbol{x}(n)C^{-1}(n) \tag{3.26}$$

The *a posteriori* estimate of the state vector and the fading process are respectively given by:

$$\widehat{\boldsymbol{h}}(n/n)=\boldsymbol{\phi}\widehat{\boldsymbol{h}}(n-1/n-1)+\boldsymbol{K}(\boldsymbol{n})\,\alpha(n) \tag{3.27}$$

and

$$\widehat{h}(n)=\hat{h}(n/n)=\boldsymbol{g}^{T}\widehat{\boldsymbol{h}}(n/n) \tag{3.28}$$

The error covariance matrix is updated as follows:

$$\boldsymbol{P}(n/n)=\boldsymbol{P}(n/n-1)-\boldsymbol{K}(n)\boldsymbol{x}^{T}(n)\boldsymbol{P}(n/n-1) \tag{3.29}$$

It should be noted that the state vector and the error covariance matrix are initially assigned to zero vector and identity matrix respectively, i.e. $\widehat{\boldsymbol{h}}(0/0)=0$ and $\boldsymbol{P}\,(0/0)=\boldsymbol{I}_{p}$.

3.5.1.4 H_{∞} Filter

Kalman filter is optimal for application with distributed Gaussian noise and ideal in the H_2 sense providing that the underlying state-space model is accurate. Really, many assumption must be satisfied in real work. Furthermore, the initial state, the driving process, and the measurement noise must be independent, white and Gaussian. Nevertheless, these assumptions not always controlled especially when used in UFMC systems, due to the uncertainties and approximations for AR process that not fit exactly fading process for lower order and noise variance and AR parameters are unknown. In [63] the H_{∞} estimation techniques, initially developed in the framework of control. On contrast, H_{∞} filtering is more

robust against the noise disturbances and modeling approximations than Kalman filtering [63]. It is principle is reducing the worst possible effects of the noise disturbances on the estimation error. Moreover, this system does not need a priori constraints on the noises, except that they have limited energies.

To estimate the fading process $\boldsymbol{h}(n)$ along the k^{th} carrier in eq. (3.32). Unlike Kalman filtering, the H_∞ filtering not only deals with the estimation of state vector $\boldsymbol{h}(n)$, but also makes it possible to focus on the estimation of specific linear combination of the state vector components as follows:

$$z(n) = \boldsymbol{l}\boldsymbol{h}(n) \tag{3.30}$$

Where l is a $1\ x\ p$ linear transformation operator. Here, as we aim at estimating the fading process h(n), the linear operator is set to be $\boldsymbol{l} = \boldsymbol{g^T} = [1\ 0\ \ldots 0]^T$. By using the state space representation of fading channel process in eq.(33-35), the proposed H_∞ filter estimate the fading process $\hat{h}(n) = \boldsymbol{l}\widehat{\boldsymbol{h}}(n)$ by minimizing the H_∞ norm of transfer operator τ that maps the noises $w(n), v(n)$ and the initial state error $\boldsymbol{e}_0 = \boldsymbol{h}(0) - \widehat{\boldsymbol{h}}(0)$ to the estimation error $e(n) = h(n) - \hat{h}(0)$as follows :

$$J_\infty = sup\, J_{w(n)v(n),h(0)} \tag{3.31}$$

Where:

$$J = \frac{\sum_{n=0}^{N-1}|e(n)|^2}{e_0^H \boldsymbol{P}_0^{-1}\boldsymbol{e}_0 + \sum_{n=0}^{N-1}(Q_w^{-1}|w(n)|^2 + R_v^{-1}\,|v(n)|^2)} \tag{3.32}$$

Where N indicates the number of data samples. While the $\boldsymbol{P}_0, Q_w > 0$ *and* $R_v > 0$ are denote to weighting parameters that are adjusted by the designer to realize the best performance requirements. Closed form expression in eq. (3.44) for optimal H_∞ not generally exist. Instead, we can use the suboptimal as the following where presented in [64]:

$$J_\infty = \gamma^2 \tag{3.33}$$

Where $\gamma > 0$ indicate for a determined disturbance attenuation level. By using this method, H_∞ Channel estimator $\hat{h}(n)$ for a given $\gamma > 0$ will be exist only in presence of stabilizing symmetric positive definite solution $\boldsymbol{P}(n)$ to the next Riccati expression:

$$\boldsymbol{P}(n+1) = \boldsymbol{\Phi P}(n)\boldsymbol{C}^{-1}(n)\boldsymbol{\Phi}^H + \boldsymbol{g}Q_w\boldsymbol{g}^T, \boldsymbol{P}(0) = \boldsymbol{P}_0 \tag{3.34}$$

Where:

$$\boldsymbol{C}(n) = \boldsymbol{I}_p - \gamma \boldsymbol{l}^T \boldsymbol{l}\boldsymbol{P}(n) + \boldsymbol{x}(n)R_v^{-1}\boldsymbol{x}^T(n)\boldsymbol{P}(n) \tag{3.35}$$

This leads to the following constraint:

$$\boldsymbol{P}(n)\boldsymbol{C}^{-1}(n) > 0 \tag{3.36}$$

If the condition in eq. (3.49) is fulfilled, the H_∞ channel estimator will exist and is given by:

$$\hat{h}(n) = \boldsymbol{l}\hat{\boldsymbol{h}}(n) \tag{3.37}$$

$$\hat{\boldsymbol{h}}(n) = \boldsymbol{\phi}\hat{\boldsymbol{h}}(n-1) + \boldsymbol{K}(n)\alpha(n), \hat{h}(0) = 0 \tag{3.38}$$

Where $\alpha(n)$ denotes for innovation process and given by:

$$\alpha(n) = r(n) - \boldsymbol{x}^T(n)\boldsymbol{\phi}\hat{\boldsymbol{h}}(n-1) \tag{3.39}$$

And $\boldsymbol{K}(n)$ denote to H_∞ gain, and given by:

$$\boldsymbol{K}(n) = \boldsymbol{P}(n)\boldsymbol{C}^{-1}(n)\boldsymbol{x}(n)R_v^{-1} \tag{3.40}$$

From previous, we notice H_∞ structure in eq. (3.47-3.53) is the same Kalman filter. But, H_∞ has more computational cost due to present condition in eq. (3.48) than Kalman filter. The H_∞ can be customized to be Kalman filter by mapping Q_w , R_v and $\boldsymbol{P}_0$ chosen to be σ_w^2 , σ_v^2

and the initial error covariance matrix of $\boldsymbol{h}(0)$ respectively. When $\gamma \to \infty$ the H_∞ filter be Kalman filter.

3.5.2 Interpolation techniques

In comb-type pilot based channel estimation, an efficient interpolation technique is necessary in order to estimate channel at data sub-carriers by using the channel information at pilot Sub-carriers. Interpolation is the process finding formula whose graph will pass through given set of points.

3.5.2.1 Linear Interpolation (LI)

The linear interpolation method was shown to perform better than the piecewise-constant interpolation [65]. It is based on approximation data at point *x* by straight line by passing through two data points. There is a unique straight line passing through these lines. The channel estimation at the data positions $k, uL < k < (u+1)L$, using interpolation is given by:

$$\hat{h}_k = \left(\hat{h}_{p_{k+1}} - \hat{h}_{p_k}\right)\frac{l}{L} + \hat{h}_{p_k}, \quad 0 \le l < L \tag{3.41}$$

where $\hat{h}_{p_k}$ is the estimated fading process at pilot symbol position.

3.5.2.2 Second Order Interpolation (SOI)

The SOI is shown fit better than linear interpolation [66]. The channel estimated by SOI is given by:

$$H_e(k) = c_1 H_p(m-1) + c_1 H_p(m) + c_{-1} H_p(m+1) \tag{3.42}$$

Where :

$$\begin{cases} c_1 = \dfrac{\alpha(\alpha-1)}{2} \\ c_0 = -\alpha(\alpha-1)(\alpha+1), \alpha = \dfrac{l}{N_1} \\ c_{-1} = \dfrac{\alpha(\alpha+1)}{2} \end{cases} \tag{3.43}$$

3.5.2.3 Low pass Interpolation (LPI)

The low-pass interpolation is implemented by adding zeros in the original sequence and later using a low pass FIR filter (interp function in MATLAB) that permits the original data to pass throughout unchanged in addition interpolates such that the mean-square error among the interpolated points and their actual values is reduced [67].

3.5.2.4 Spline Cubic Interpolation (SCI)

The spline cubic interpolation (spline function in MATLAB) gives a soft and continuous polynomial fitted to particular data points [67]. It is based on drawing smooth curves through a number of points. The (spline function in Matlab) used to generate smooth curves.

3.5.3 Fading channel equalization

Once the fading process at pilot and data symbols were estimated using the proposed approach, channel equalization could be performed by multiplying equation (2.32) with a normalized version of the complex conjugate of the channel estimate as follows:

$$\hat{\boldsymbol{x}}_k(n) = \boldsymbol{Y}_k(n)\left(\frac{\hat{h}_k^*(n)}{\left|\hat{h}_k(n)\right|^2}\right) \tag{3.44}$$

Chapter 4

Simulation Results

4.1 Simulation environment

In this chapter, we performed a comparative simulation study on the estimation of the UFMC fading channels between conventional filters like LMS, RLS, Kalman and H_∞ filters based estimators. Furthermore, we examine the performance of interpolation techniques like linear, low pass and spline. Additionally, we test the effect of the number of pilot symbols N_p on the BER performance. The UFMC wireless system is implemented and simulated using MATLAB to allow various parameters of the system to be varied and tested.

In all of our simulations, the fading channels are generated according to the autoregressive model based in [60]. The autoregressive model order p is set to $p = 2$. The step size for the LMS algorithm is set to $\mu = 0.03$ and the forgetting factor for RLS algorithm is set to $\lambda = 0.4$.

4.2 QAM Modulation

UFMC system still use QAM modulation as it retains the complex orthogonality, which works with existing MIMO schemes. We test QAM modulation techniques for different

values of bits per subcarriers. Since the bits are mapped to a subcarrier amplitude and phase, which is represented by a complex in phase and quadrature phase (I-Q) vector. The number of points on the constellation is indicated in the modulation format description (4QAM uses 4-point constellation). Figure (4.1) shows the BER performance of UFMC using different mapping techniques over Rayleigh channel. It is clear that the best QAM modulation when we use the Bits per subcarrier (2). 4-QAM is achieves greater distance between adjacent points in the I-Q plane by distributing the points more evenly. In this way, the points on the constellation points are more distinct and data errors are reduced.

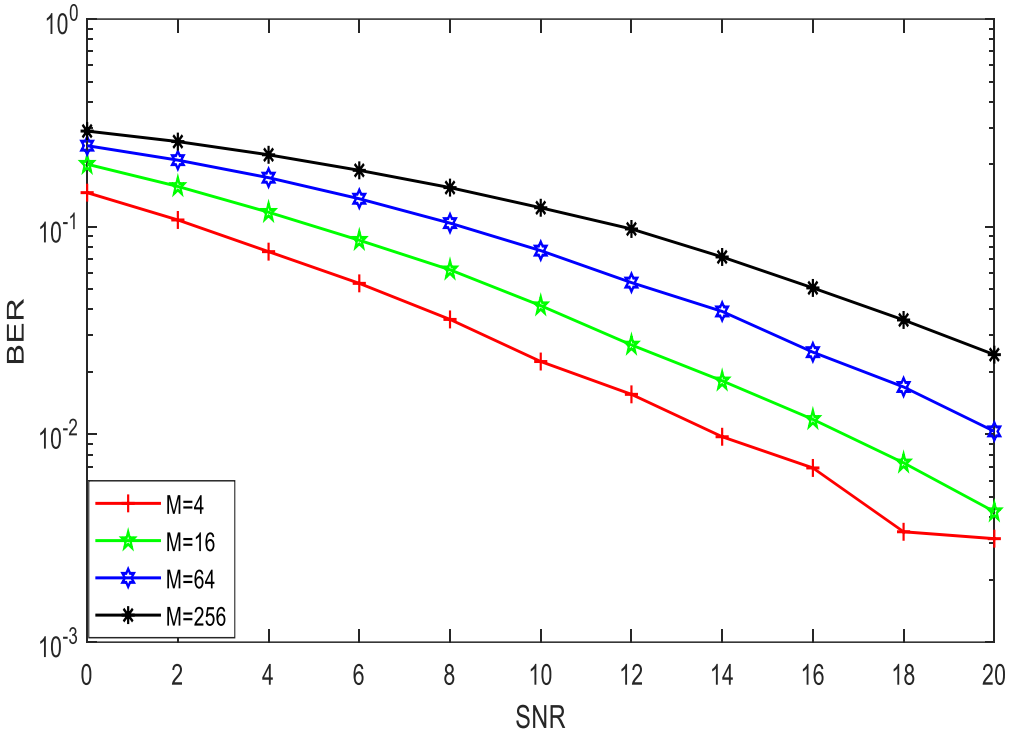

Figure 4: 1: BER vs SNR for UFMC QAM Modulation.

4.3 **UFMC Channel Envelope and Phase**

In this section, we want to study the envelope and phase of the estimated fading process using various channel estimator with low pass interpolation. When using different adaptive filters with Doppler rate $f_d T_s = 0.1111$, M=2048, $N_p = 256$, SNR=15dB. Figure 4.2 and 4.3

respectively shows the envelope and phase of the estimated fading process using the various channel estimators. The main advantage of Rayleigh fading generator is the samples of fading sequence can be generated as they required. The complex fading process h(n) has looping quasi-periodic behavior. Especially at low amplitude, h(n) exhibits rapid phase changes when it traverse close to the origin. Phase inversions usually when the signal is the weakest and the SNR the poorest. One can notice that the H_∞ filter based estimator provides better estimation than LMS, RLS and Kalman, particularly at deep fading.

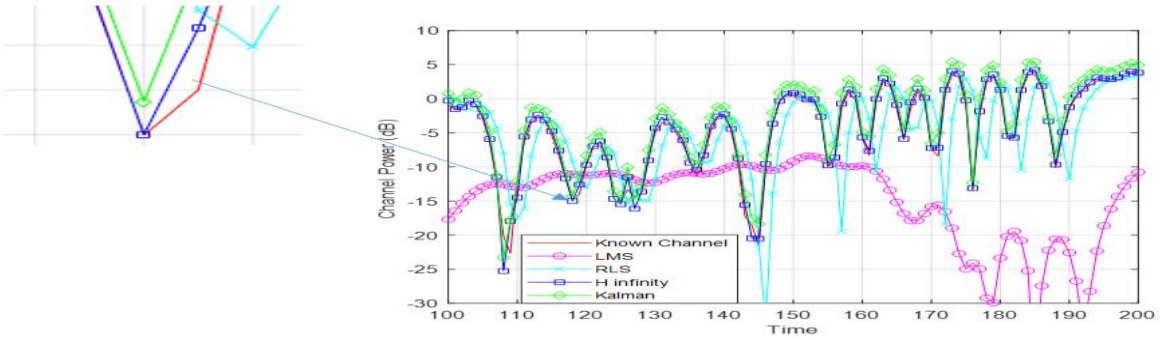

Figure 4: 2: Envelope of estimated fading process using the various estimators

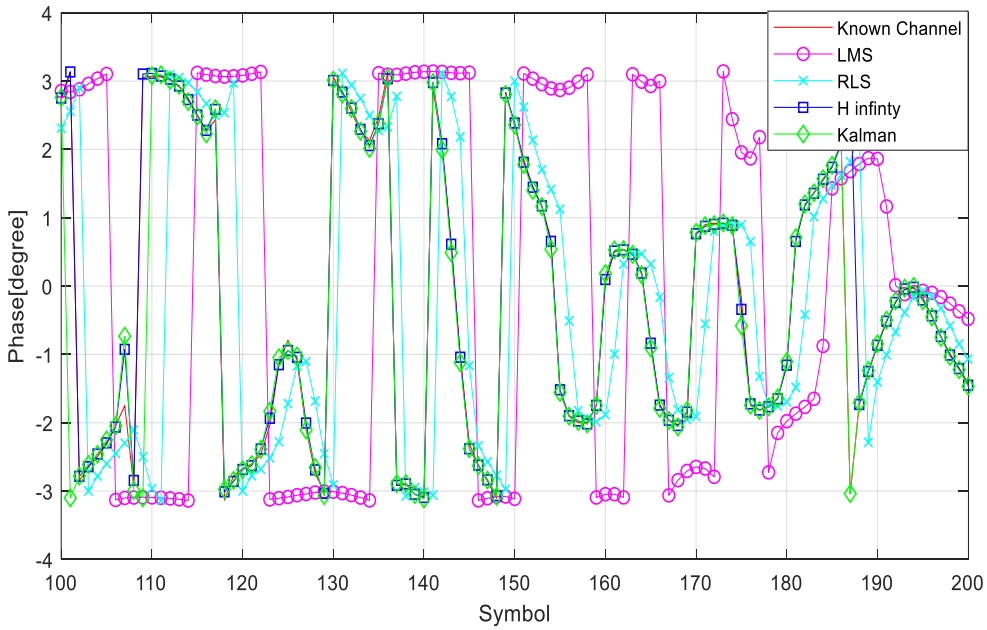

Figure 4: 3: Phase of estimated fading process using the various estimators

4.4 **BER performance versus SNR**

Figures (4.4-4.6) shows the BER performance versus SNR for the UFMC system when using various channel estimators with $M = 2048, N_p = 256$ pilots with different values of Doppler $f_d T_s = 0.1111$, $f_d T_s = 0.0741$, $f_d T_s = 0.0370$ and respectively, using low-pass interpolation. According to figures (4.4-4.5), the proposed H_∞ based estimator outperforms the LMS,RLS and Kalman filter with performance difference increases as the SNR increases when we us. for high and medium Doppler rate. According to figure (4.6), performance of H_∞ is the same for Kalman filter for lower Doppler rate. In addition, the performance of RLS estimator is improved when use lower Doppler rate.

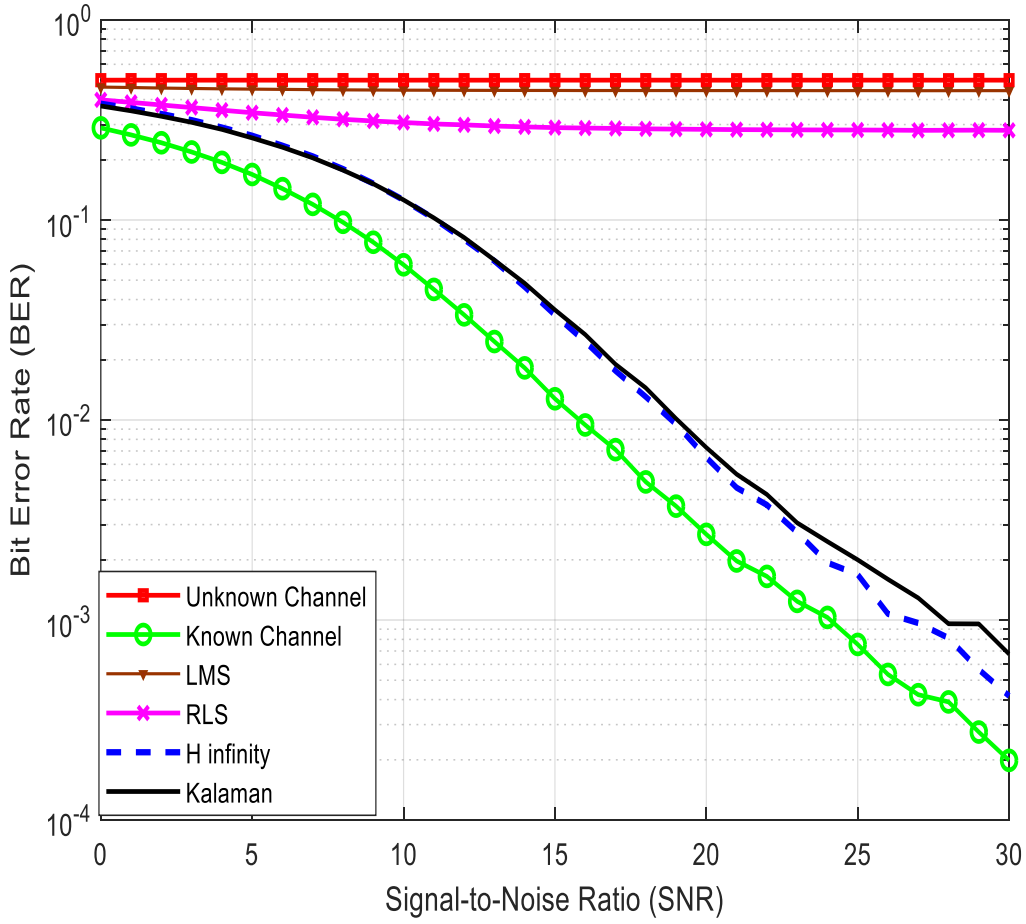

Figure 4: 4: BER performance vs SNR for UFMC system with various channel estimators. $f_d T_s = 0.1111$

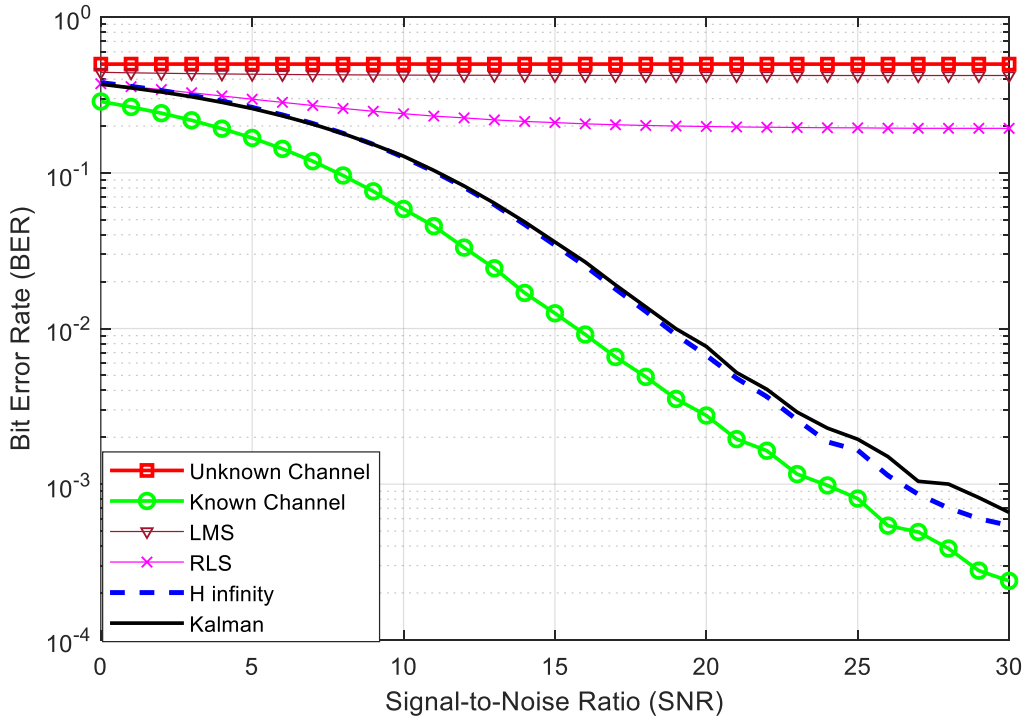

Figure 4: 5: BER performance vs SNR for UFMC system with various channel estimators.

$f_d T_s = 0.0741$

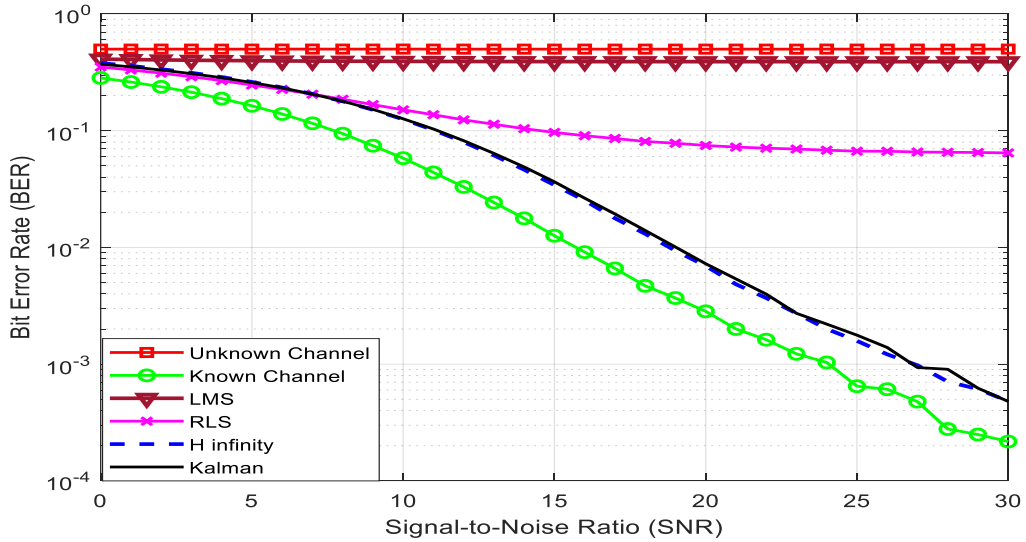

Figure 4: 6: BER performance vs SNR for UFMC system with various channel estimators.

$f_d T_s = 0.037$

Figure (4.7) displays the BER performance of the UFMC system when using H_∞ filter with various interpolation techniques, M=2048, $N_p = 256$ and $f_d T_s = 0.0741$. it is confirmed that the low pass interpolation yields the best BER performance.

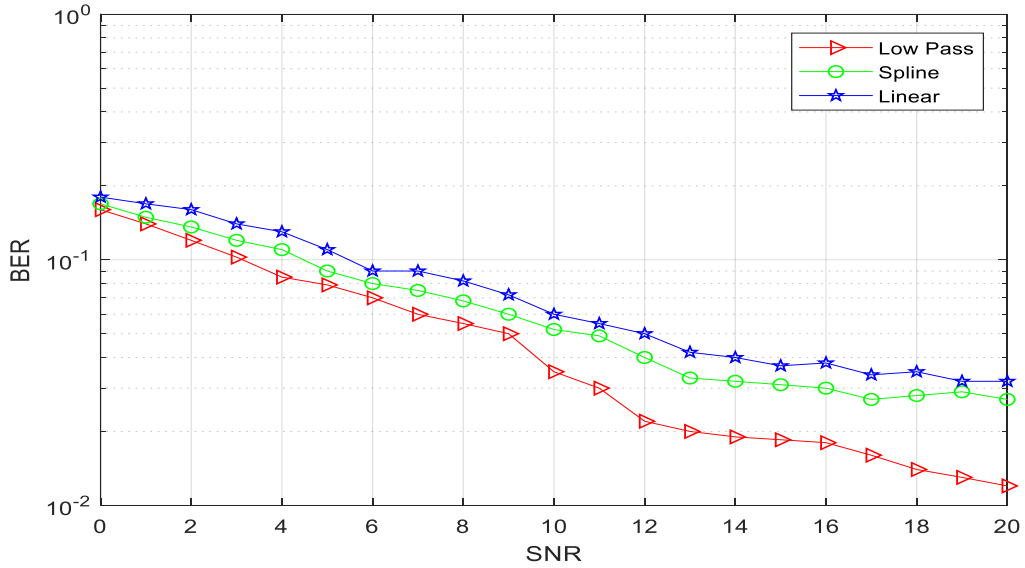

Figure 4: 7: BER performance vs SNR for UFMC system with the various using interpolation methods. $M = 2048$, $N_p = 256$, and $f_d T_s = 0.0741$.

Figure (4.8) shows the effect of changing the number of pilot symbols N_p on the BER performance of the UFMC system when using H_∞ filter based channel estimator with low-pass interpolation. Indeed, increasing the number of pilot symbols N_p will improve the BER performance of the system.

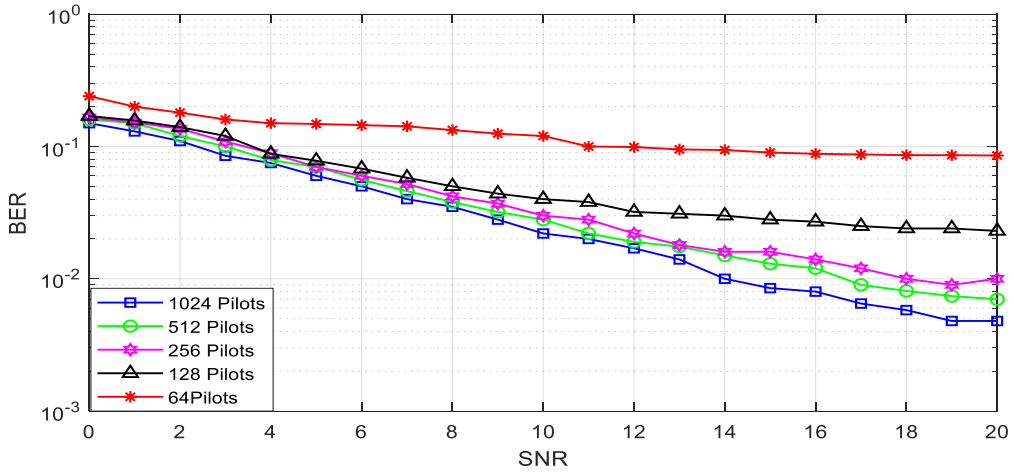

Figure 4: 8: BER performance vs SNR for UFMC system with different numbers of pilot symbols various when using $\boldsymbol{H}_\infty$ interpolation methods. $M = 2048$, $N_p = 256$, and $f_d T_s = 0.0741$.

Chapter 5

Conclusion and Future Work

5.1 Conclusion

UFMC modulation system is a very strong candidate for future mobile generation 5G. It combines between advantages of OFDM and FBMC and avoided their drawbacks. It achieves high data rate and high power spectral density than other modulation systems. Also, it solves the fixed synchronization problem in current modulation system and supports new applications like IOT, D2D, V2V, M2M and a large number of smart devices.

We address the estimation and equalization of UFMC fading channels based on comb pilot symbols arrangement. The estimation process is dived to two stages. The first stage is estimation fading channel by an adaptive filter like H_∞, Kalman, RLS, and LMS filters. The second stage is the interpolation at data symbol position by various techniques like linear, Low pass, spline, Second order and time domain. The simulation results showed the performance of the H_∞ filter-based estimator outperforms than LMS and RLS and Kalman. Indeed, the H_∞ filters based estimator can exploit the fading channel statistics and can track fast variations of rapidly varying fading channels. In addition, the low-pass interpolation is confirmed to outperform both spline and linear interpolation.

5.2 **Future Work**

At the end of this thesis, several problems can be suggested for future work. They can be pointed out as below:

- We have studied the estimation of the fading process in case of flat fading. In the future, we can extend the work for estimation the fading process in case of frequency selective fading.
- We have used only comb-pilot arrangement for channel estimation. Possible future work can investigate the relevance of other pilot arrangements such as block or rectangular pilot arrangements for channel estimation with decision feedback.
- We address the estimating of fading process only by H_∞ filters. So we can extend the work to make a joint estimation for fading process and AR parameters by using a couple of H_∞ or Kalman filters.
- We have assumed that the fading processes over all carriers are uncorrelated and, hence, they are estimated separately. However, the correlation among multi-carrier fading processes might arise due to the existence of a significant Doppler spread for instance. To exploit these correlations, the joint estimation of the fading processes can be addressed based on a vector (multi-channel) AR model. Therefore, the extension of the proposed channel estimation techniques to account for a vector AR model is a possible direction for future work.

Acronyms and Abbreviation

0G: Zero Generation

1G: First Generation

2G: Second Generation

3G: Third Generation

4G: Fourth Generation

5G: Fifth Generation

ADSL: Asymmetric Digital Subscriber Line

ACF: Autocorrelation Function

AR: Autoregressive Model

AWGN: Additive White Gaussian Noise

BER: Bit Error Rate

CP: Cyclic Prefix

CFO: Carrier Frequency Offset

CP-OFDM: Cyclic Prefix Orthogonal Frequency Division Multiplexing

CSI: Channel State Information

DAB: Digital Audio Broadcasting

DVB: Digital Video Broadcasting

D2D: Device to Device

DFT: Discrete Fourier Transform

DFTI: Discrete Fourier Transform Interpolation

FBMC: Filter Bank Multicarrier

FFT: Fast Fourier Transforms

FIR: Finite Impulse Response

G: Generation

GSM: Global System of Mobile

GPRS: General Packet Radio Service

H_∞: H Infinity Filter

ICI: Inter-Carrier Interference

IFFT: Inverse Fast Fourier Transforms

ISI: Inter-Symbol Interference

IoT: Internet of Things

ISBI: Inter Symbol Band Interference

IIR: Infinite Impulse Response

I.I.D: Independent and Identically Distribution

IDFT: Inverse Discrete Fourier Transform.

LMS: Least Mean Square

LS: Least Square

LTE: Long Term Evolution

LSLI: Linear Square Linear Interpolation

Ls: Least Square.

LI: Linear Interpolation

LPI: Low Pass Interpolation

LOS: Line of Sight

MCM: Multicarrier Modulation

MTC: Multi-Machine

MIMO: Multiple Input Multiple Output

MC: Multi-Carrier

MMSE: Minimum Mean Square Error

MSE: Mean Square Error

NLOS: No Line of Sight

OFDM: Orthogonal Frequency Division Multiplexing

OOB: Out of Band

P/S: Parallel to Serial

PSD: Power Spectrum Density

PARP: Peak to Average Power Ratio

PDF: Probability Density Function.

QAM: Quadrature Amplitude Modulation

RLS: Recursive Least Square

RMMSE: Relaxed Minimum Mean Square Error

SMS: short Message Service

S/P: Serial to Parallel

SOI: Secondary Order Interpolation.

SCI: Spline Cubic Interpolation

SOS: Sum of Sinusoids

TDI: Time Domain Interpolation

UFMC: Universal Filter Multi-carrier

UWB: Ultra Wideband

V2V: Vehicle to Vehicle

WiMAX: Worldwide Interoperability for Microwave Access

WLAN: Wireless Local Area Networks

WIFI: Wireless Fidelity

WMAN: Wireless Metropolitan. Area Network

WSS: Wide Sense Stationary

YWE: Yule-Walker Equation

Notations

$\hat{h}_k(n)$: Estimated fading channel

$h_k(n)$: Fading channel along subcarriers at symbol n

$\hat{h}_{k+1}$: Channel estimator at tab K+1

$\hat{h_0} = zeros(p)$: Initial parameters of order p

$\hat{h}_{0/0}$**:** Initial state Vector

$J_0(.)$: Zero order Bessel function

L_s: Number of scatters

R_k: Autocorrelation function

T_s*:* Sampling interval period

$f_d T_s$: Doppler rate

f_d: Doppler frequency

f_s *:* Sampling rate

$s_k(n)$: Signal at the input of channel estimation and equalization

$n_k[n]$: AWGN signal

K_{a_k} : Kalman gain

P_a: Error covariance matrix

$\theta_k(n)$: Phase mapping between real data sequence and complex samples

M*:* Overall number of subcarriers, FFT size

R : Fading channel autocorrelation matrix

$S(f)$: Power spectrum density function

$g(ml)$: Random scattered amplitude

k *:* Subcarrier index ($k = 0, \dots, M-1;\ k = 0$ corresponds to center subcarrier)

l : Linear Transformation operator

$r(m)$: Received signal

v : Mobile speed

$y(m)$: Transmitted signal

λ : Forgetting factor of RLS

λ: Wave length of the carrier wave

μ: LMS step size

$\varphi(ml)$: Angle of arrival

$\vartheta(ml)$: Initial phase

ϕ : Transition matrix

$w_R(n)$: Rectangular Window Weight Function

L: Length of Window Filter

$w_c(n)$: Raised Cosine Function

$w_h(n)$: Hamming Weight Function

σ: Variance

$W_{0,k}$: Zero Phase Dolph Chebyshev Window

α: Parameter to adjust side lobe level

B: Subbnad

S_k: Frequency Complex Symbol

$x_k[n]$: Base Band Signal

K: k^{th} carrier

m^{th} : UFMC symbol at m=1, 2,3,…M-1

$p_R(r)$: Probability Density Function

Ω: Variance

$S(f)$: Power Spectral Density

f_d: Maximum Doppler Frequency

$r_k[n]$: Received Signal

$\delta(t)$: Dirac Pulse

τ_n: Time delay

$\rho_n e^{j\Phi_n}$: Complex amplitude (Amplitude and Phase) of the received pulses

$p(x;\sigma)$: Probability Density Function

$\upsilon(n)$: Complex white Gaussian noise process with uncorrelated real and imaginary elements

${\sigma_\upsilon}^2$: Variance of Driving Process

f_n : Normalized Frequency

R_k^{mod}: Modified Correlation Function

p: Autoregressive Model Order

θ : Vector of AR Parameters

N_p : Inserted pilots

F: Cost Function

P_0: Identity Matrix

C_k: Variance of Innovation Process

$P_{k/k-1}$: *a priori* error covariance matrix

$\hat{h}_{k/k}$: *a posteriori* estimate

$P_{k/k}$: Error covariance matrix

$H\infty$: H infinity Filter

e_k: Estimation Error

e_0: Initial State Error

γ: Level of disturbance attenuation

Q_w : Weighting Parameters

R_v: Weighting Parameters

$\hat{x}_k(n)$: Symbol estimate

Bibliography

[1] Bhalla, Mudit Ratana, and Anand Vardhan Bhalla. "Generations of mobile wireless technology: A survey." International Journal of Computer Applications 5, no. 4 (2010).

[2] Black, Uyless D., and Ulyess Black. Second generation mobile and wireless networks. NJ: Prentice Hall, 1999.

[3] Juha, Korhonen. "Introduction to 3G mobile communications." Artcch. House (2003).

[4] Rahman, M., and F. A. M. Mir. "Fourth Generation (4G) mobile networks-features, technologies & issues." In 3G and Beyond, 2005 6th IEE International Conference on, pp. 1-5. IET, 2005.

[5] Sood, Roopali, and Atul Garg. "Digital society from 1G to 5G: a comparative study." International Journal of Application or Innovation in Engineering & Management (IJAIEM) 3, no. 2 (2014): 186-193.

[6] Steveperky, https://www.steveperky.com/digital-age-welcomes-pope-francis-i/

[7] Cisco,https://www.cisco.com/c/en/us/solutions/collateral/service-provider/visual-networking-index-vni/mobile-white-paper-c11-520862.html

[8] Aldababseh, Mahmoud, and Ali Jamoos. "Estimation of FBMC/OQAM fading channels using dual Kalman filters." The Scientific World Journal 2014 (2014).

[9] Goldsmith, Andrea. Wireless communications. Cambridge university press, 2005.

[10] 3gpp, http://www.3gpp.org/news-events/3gpp-news/1831-sa1_5g

[11] Li, Ye Geoffrey, and Gordon L. Stuber, eds. Orthogonal frequency division multiplexing for wireless communications. Springer Science & Business Media, 2006.

[12] Baum, Kevin, Brian Classon, and Phillire Sartori. Principles of broadband OFDM cellular system design. Wiley, 2008.

[13] Farhang-Boroujeny, Behrouz. "OFDM versus filter bank multicarrier." IEEE signal processing magazine 28, no. 3 (2011): 92-112.

[14] Zhang, Haijian, Didier Le Ruyet, Daniel Roviras, Yahia Medjahdi, and Hong Sun. "Spectral efficiency comparison of OFDM/FBMC for uplink cognitive radio networks." EURASIP Journal on Advances in Signal Processing 2010 (2010).

[15] G. Bochechka. “Methods of channel estimation based on built in pilot-signals in OFDM systems” Telecommunications and Transport, 2009, No3, pp. 38-42.

[16] G. Bochechka, Estimation of the beginning of the OFDM block and frequency shift in system IEEE 802.11a.T-Comm Telecommunications and Transport, 2009, №5, pp.34-37.

[17] Hu, Fei, ed. Opportunities in 5G networks: A research and development perspective. CRC Press, 2016.

[18] ‘‘More than 50 billion connected devices,’’ Ericsson, Stockholm, Sweden, White Paper 284 23-3149, Feb. 2011. [Online]. Available: http://www.akosrs.si/files/Telekomunikacije/Digitalna_agenda/Internetni_protokol_Ipv6/More-than-50-billion-connected-devices.pdf.

[19] Wang, Rong, Jingye Cai, Xiang Yu, and Sirui Duan. "Compressive channel estimation for universal filtered multi-carrier system in high-speed scenarios." IET Communications 11, no. 15 (2017): 2274-2281.

[20] Geng, Suiyan, Xin Xiong, Linlin Cheng, Xiongwen Zhao, and Biao Huang. "UFMC system performance analysis for discrete narrow-band private networks." In Microwave, Antenna, Propagation, and EMC Technologies (MAPE), 2015 IEEE 6th International Symposium on, pp. 303-307. IEEE, 2015.

[21] Gökceli, Selahattin, and Buse Canli. "Universal filtered multicarrier systems: Testbed deployment of a 5G waveform candidate." In *Sarnoff Symposium, 2016 IEEE 37th*, pp. 94-99. IEEE, 2016.

[22] Ozdemir, Mehmet Kemal, and Huseyin Arslan. "Channel estimation for wireless OFDM systems." *IEEE Communications Surveys & Tutorials* 9, no. 2 (2007): 18-48.

[23] Jamoos, Ali, Ahmad Abdo, Hanna Abdel Nour, and Eric Grivel. "Two cross-coupled H∞ filters for fading channel estimation in OFDM systems." In Novel Algorithms and Techniques in Telecommunications and Networking, pp. 349-353. Springer, Dordrecht, 2010.

[24] Jamoos, Ali, Ahmad Abdo, and Hanna Abdel Nour. "Estimation of OFDM time-varying fading channels based on two-cross-coupled Kalman filters." In Novel Algorithms and Techniques In Telecommunications, Automation and Industrial Electronics, pp. 287-292. Springer, Dordrecht, 2008.

[25] Jamoos, Ali, Eric Grivel, Nicolai Christov, and Mohamed Najim. "Estimation of autoregressive fading channels based on two cross-coupled H∞ filters." Signal, image and video processing 3, no. 3 (2009): 209-216.

[26] Jamoos, Ali, Eric Grivel, Nidal Shakarneh, and Hanna Abdel Nour. "Dual H∞ vs dual Kalman filters for M-AR parameter estimation from noisy observations." In Signal Processing Conference, 2009 17th European, pp. 1700-1704. IEEE, 2009.

[27] Jamoos, Ali, Eric Grivel, N. Shakarneh, and H. Abdel-Nour. "Dual optimal filters for parameter estimation of a multivariate autoregressive process from noisy observations." IET Signal Processing 5, no. 5 (2011): 471-479.

[28] Driggs, Jonathan, Taylor Sibbett, Hussein Moradi, and Behrouz Farhang-Boroujeny. "Channel estimation for filter bank multicarrier systems in low SNR environments." In Communications (ICC), 2017 IEEE International Conference on, pp. 1-7. IEEE, 2017.

[29] Kofidis, Eleftherios, Dimitrios Katselis, Athanasios Rontogiannis, and Sergios Theodoridis. "Preamble-based channel estimation in OFDM/OQAM systems: A review." Signal Processing 93, no. 7 (2013): 2038-2054.

[30] Kofidis, Eleftherios, and Dimitrios Katselis. "Improved interference approximation method for preamble-based channel estimation in FBMC/OQAM." In Signal Processing Conference, 2011 19th European, pp. 1603-1607. IEEE, 2011.

[31] Chen, Chih-Wei, and Fumiaki Maehara. "An enhanced MMSE subchannel decision feedback equalizer with ICI suppression for FBMC/OQAM systems." In Computing, Networking and Communications (ICNC), *2017 International Conference on*, pp. 1041-1045. IEEE, 2017.

[32] Stitz, Tobias Hidalgo, Tero Ihalainen, Ari Viholainen, and Markku Renfors. "Pilot-based synchronization and equalization in filter bank multicarrier communications." EURASIP Journal on Advances in Signal Processing 2010 (2010): 9.

[33] Wang, Xiaojie, Thorsten Wild, Frank Schaich, and Stephan ten Brink. "Pilot-aided channel estimation for universal filtered multi-carrier." In Vehicular Technology Conference (VTC Fall), 2015 IEEE 82nd, pp. 1-5. IEEE, 2015.

[34] Zhang, Lei, Chang He, Juquan Mao, Ayesha Ijaz, and Pei Xiao. "Channel estimation and optimal pilot signals for universal filtered multi-carrier (UFMC) systems." In Personal, Indoor, and Mobile Radio Communications (PIMRC), 2017 IEEE 28th Annual International Symposium on, pp. 1-6. IEEE, 2017.

[35] Wang, Rong, Jingye Cai, Xiang Yu, and Sirui Duan. "Compressive channel estimation for universal filtered multi-carrier system in high-speed scenarios." IET Communications 11, no. 15 (2017): 2274-2281.

[36] Jamoos, Ali, and Moataz Hussein. "Estimation of UFMC Time-Varying Fading Channel Using Adaptive Filters." In 2018 International Conference on Promising Electronic Technologies (ICPET), pp. 43-48. IEEE, 2018.

[37] Harris, Fredric J. "On the use of windows for harmonic analysis with the discrete Fourier transform." Proceedings of the IEEE 66, no. 1 (1978): 51-83.

[38] Parks, Thomas W., and C. Sidney Burrus. Digital filter design. Wiley-Interscience, 1987.

[39] Dogra, Shushank, and Narinder Sharma. "Comparison of Different Techniques to Design of Filter." International Journal of Computer Applications (0975–8887) Volume (2014).

[40] Saramäki, Tapio, S. K. Mitra, and J. F. Kaiser. "Finite impulse response filter design." Handbook for digital signal processing 4 (1993): 155-277.

[41] Nuttall, Albert. "Some windows with very good sidelobe behavior." IEEE Transactions on Acoustics, Speech, and Signal Processing 29, no. 1 (1981): 84-91.

[42] Toraichi, K.; Kamada, M.; Itahashi, S.; Mori, R. (1989). "Window functions represented by B-spline functions". IEEE Transactions on Acoustics, Speech, and Signal Processing. 37: 145. doi:10.1109/29.17517.

[43] Dolph, C. L. "A current distribution for broadside arrays which optimizes the relationship between beam width and side-lobe level." Proceedings of the IRE 34, no. 6 (1946): 335-348.

[44] Bochechka, Grigory, Valery Tikhvinskiy, Ivan Vorozhishchev, Altay Aitmagambetov, and Bolat Nurgozhin. "Comparative analysis of UFMC technology in 5G networks." In Control and Communications (SIBCON), 2017 International Siberian Conference on, pp. 1-6. IEEE, 2017.

[45] Zhang, Lei, Chang He, Juquan Mao, Ayesha Ijaz, and Pei Xiao. "Channel estimation and optimal pilot signals for universal filtered multi-carrier (UFMC) systems." In Personal, Indoor, and Mobile Radio Communications (PIMRC), 2017 IEEE 28th Annual International Symposium on, pp. 1-6. IEEE, 2017.

[46] https://www.slideshare.net/ShreeKrupa1/multichannel-fading

[47] WC Jr, Jakes. "Microwave mobile communications." (1974).

[48] Ozdemir, Mehmet Kemal, and Huseyin Arslan. "Channel estimation for wireless OFDM systems." IEEE Communications Surveys & Tutorials 9, no. 2 (2007): 18-48.

[49] Prasad, Ramjee. OFDM for wireless communications systems. Artech House, 2004.

[50] Van De Beek, J-J., Ove Edfors, Magnus Sandell, Sarah Kate Wilson, and P. Ola Borjesson. "On channel estimation in OFDM systems." In Vehicular Technology Conference, 1995 IEEE 45th, vol. 2, pp. 815-819. IEEE, 1995.

[51] Hsieh, Meng-Han, and Che-Ho Wei. "Channel estimation for OFDM systems based on comb-type pilot arrangement in frequency selective fading channels." IEEE Transactions on Consumer Electronics 44, no. 1 (1998): 217-225.

[52] Steele, Raymond, H. Ahmadi, and A. Krishna. "Mobile radio communications." In IEEE Proceedings, vol. 82, no. 9, pp. 1468-1468. [New York, NY]: Institute of Electrical and Electronics Engineers, 1963-, 1994.

[53] Farhang-Boroujeny, Behrouz. "A square-root Nyquist (M) filter design for digital communication systems." IEEE Transactions on Signal Processing 56, no. 5 (2008): 2127-2132.

[54] Eghbali, Amir, and Håkan Johansson. "On Efficient Design of High-Order Filters with Applications to Filter Banks and Transmultiplexers with Large Number of Channels." IEEE Trans. Signal Processing 62, no. 5 (2014): 1198-1209.

[55] Wen, Jiangang, Jingyu Hua, Sunan Li, Kai Zhou, and Dongming Wang. "Interference-driven designs of nonlinear-phase FIR filter with application in FBMC system." China Communications 13, no. 12 (2016): 15-24.

[56] Young, David J., and Norman C. Beaulieu. "The generation of correlated Rayleigh random variates by inverse discrete Fourier transform." IEEE Transactions on Communications 48, no. 7 (2000): 1114-1127

[57] Loo, Chun, and Norman Secord. "Computer models for fading channels with applications to digital transmission." IEEE Transactions on Vehicular Technology 40, no. 4 (1991): 700-707.

[58] Hoeher, Peter. "A statistical discrete-time model for the WSSUS multipath channel." IEEE Transactions on vehicular technology 41, no. 4 (1992): 461-468.

[59] Verdin, D., and T. C. Tozer. "Generating a fading process for the simulation of land-mobile radio communications." Electronics Letters 29, no. 23 (1993): 2011-2012.

[60] Pop, Marius F., and Norman C. Beaulieu. "Limitations of sum-of-sinusoids fading channel simulators." IEEE Transactions on Communications 49, no. 4 (2001): 699-708.

[61] Baddour, Kareem E., and Norman C. Beaulieu. "Autoregressive modelling for fading channel simulation." IEEE Transactions on Wireless Communications 4, no. 4 (2005): 1650-1662.

[62] Kay, Steven M. *Modern spectral estimation*. Pearson Education India, 1988.

[63] Coleri, Sinem, Mustafa Ergen, Anuj Puri, and Ahmad Bahai. "Channel estimation techniques based on pilot arrangement in OFDM systems." IEEE Transactions on broadcasting 48, no. 3 (2002): 223-229.

[64] Hassibi, Babak, Ali H. Sayed, and Thomas Kailath. Indefinite-Quadratic Estimation and Control: A Unified Approach to H2 and H-infinity Theories. Vol. 16. SIAM, 1999.

[65] Shen, X-M., and Li Deng. "Game theory approach to discrete H/sub/spl infin//ilter design." IEEE Transactions on Signal Processing 45, no. 4 (1997): 1092-1095.

[66] Cimini, Leonard. "Analysis and simulation of a digital mobile channel using orthogonal frequency division multiplexing." IEEE transactions on communications 33, no. 7 (1985): 665-675.

[67] Hsieh, Meng-Han, and Che-Ho Wei. "Channel estimation for OFDM systems based on comb-type pilot arrangement in frequency selective fading channels." IEEE Transactions on Consumer Electronics 44, no. 1 (1998): 217-225.

مشاركة حول تقدير القنوات المضمحلة للجيل الخامس (5G) من أنظمة الاتصالات الخليوية

إعداد: معتزحسين علي قرعوش

إشراف: د. علي جاموس

الملخص

يجمع النظام المقترح المبني على الفلتر العالمي متعدد الناقلات (UFMC) والمرشح للاستخدام في أنظمة الجيل الخامس (5G) للاتصالات الخليوية بين فوائد وميزات الانظمة المستخدمة حاليا في الجيل الرابع ومنها (OFDM) و (FBMC)، و تجنب مساوئ هذه الانظمة من أجل تحقيق معدل عالي في نقل البيانات ودعم تطبيقات جديدة والازدياد المتسارع في الأجهزة الذكية المباعة في الاسواق. يهدف هذا البحث حل مشكلة تقدير التغيرات في قنوات الاتصال المضمحلة للنظام اللاسلكي (UFMC) اعتمادا على ارسال رموز معروفة مسبقا لدى المستقبل. الحلول التقليدية او الأساسية تتم باستخدام طريقتي الأقل تربيع (LS) و متوسط الحد الأدنى لخطأ التربيع (MMSE) ومن ثم تطبيقها على المرشحات المتكيفة التقليدية (LMS and RLS) إضافة الى المرشحات المثلى (H_∞ and Kalman). ويمكن الاستفادة من الخصائص الإحصائية للقنوات من خلال استخدام نموذج الانحدار الذاتي ليمثل القنوات المضمحلة (Autoregressive model) وهذا النموذج يحتاج إلى معرفة بعض المعاملات، والتي يمكن تقديرها من خلال حل معادلات Yule-Walker Equations.

تتم عملية تقدير القناة المضمحلة على مرحلتين: ففي المرحلة الاولى يتم تقدير القناة المضمحلة التابعة للرموز الاستطلاعية باستخدام المرشحات (LMS, RLS, Kalman and H_∞ filters). وفي المرحلة الثانية: يتم تقدير القناة للرموز التي تعبر عن المعلومات باستخدام طرق الاستيفاء (Interpolation) مثل استيفاء التمرير المنخفض (Low Pass Interpolation والاستيفاء الخطي (Linear interpolation) واستيفاء الشريحةInterpolation) (Spline.

تم بناء نظام (UFMC) باستخدام برنامج الماتلاب (Matlab 2017) وتم عمل محاكاة للمرسل والمستقبل والقنوات وتحليل النتائج. حيث تبين أن معدل الخطأ (BER) للمرشحات المقترحة (Kalman, H_∞) أفضل من معدل الخطأ للمرشحات الأخرى وكذلك معدل الخطأ لطريقة استيفاء التمرير المنخفض (Low Pass Interpolation) أقل من معدل الخطأ للطرق الاخرى.

Appendix: Published paper in IEEE Xplore Digital Library

ICPET2018

2018 International Conference on Promising Electronic Technologies - ICPET

3 Oct-4 Oct 2018 Palestine Technical College-Deir El-Balah, Palestine

https://ieeexplore.ieee.org/document/8531227

Estimation of UFMC Time-Varying Fading Channel Using Adaptive Filter

Ali Jamoos
Department of Electronic and Communication Engineering
Al-Quds University
Jerusalem, Palestine
ali.jamoos@staff.alquds.edu

Moataz Hussein
Information and Communication Technology Center
Al-Quds Open University
Jerusalem, Palestine
moataz@qou.edu

Abstract **– Universal filtered multicarrier (UFMC) modulation technique was suggested as a strong candidate system for future 5G mobile communication systems. Indeed, it combines the advantages of orthogonal frequency division multiplexing (OFDM) and filter bank multicarrier (FBMC) modulation techniques while avoids their drawbacks. UFMC seems to be more effective for future 5G applications and scenarios like a machine to machine (M2M), vehicle to vehicle (V2V), device to device (D2D) and the Internet of Things (IoT). This paper address the estimation and equalization of UFMC time-varying fading channels using adaptive filters based on comb pilot symbols arrangement. To exploit the fading channel statistics, the fading process evolution is modeled by an autoregressive (AR) model and tracked by a Kalman filter. The AR model parameters are obtained by solving the so-called Yule-Walker (YWE) equations based on the Bessel autocorrelation function of the fading channel with known Doppler rate. The result of MATLAB simulation show the effectiveness of the proposed Kalman filter based channel estimator as compared with the conventional ones like recursive least square (RLS) and least mean square (LMS) channel estimator.**

Keywords**— UFMC, fading channel, channel estimation, pilot symbols, Kalman filter, Autoregressive model.**

I. INTRODUCTION

The current multiple access in a 4G mobile generation is OFDM which is widely employed in Power Line communication, , UWB, ADSL, Digital Audio broadcasting (DAB), digital video broadcasting (DVB), and WLAN standards, Wireless metropolitan network (WMAN) and WiMAX [1,2]. The advantages of OFDM is easy transceiver implementation where it is performed using pair of (IFFT, FFT) at transmitter and receiver respectively. The implementation of pair is very easy by digital processing [3, 4].

However, it had many drawbacks and restrictions like cyclic prefix(CP), high overhead, higher sensitivity to carrier frequency offset (CFO) and phase variance of the received signal related to the reference at receiver [5,6], high Peak average power ratio (PARP) which reduces the power of transmitter and relatively low spectral power density (PSD). FBMC is short for filter bank multicarrier modulation technique. It one of possible system candidate to be employed in future 5G. The implementation of FBMC is the same OFDM system based on IFFT/FFT pairs operation, and it used a bank of digital filters like: prototype filter instead of guard interval with a cyclic prefix to raise spectral efficiency compared to OFDM especially when it combines with offset quadrature amplitude modulation (OQAM). It uses digital filtering to solve sensitivity interference between adjacent subcarriers, less sensitive to CFO, more clearer carriers, more resistance to estimation error due to time/frequency shift by removing or elimination of sidelobes.

Due to all mentioned limitations, and the vision of 5G to serve wide different smart mobiles, extreme Mobile broadband, massive M2M, IoT, V2V, D2D [7-9]. The key design of candidate system modulation technique is flexibility, versatility, scalability, and efficiency to serve wide range of applications access [8, 9]. Supporting M2M is big challenging feature of 5G , it will be serve around 50 billion machines that expected to be connected by the year 2020 [10]. Hence, for 5G, BER performance for proposed schemes better than current system are under study [11, 12]. Some candidate's schemes like FBMC [13], and Generalized Frequency Division Multiplexing (GFDM) [14] and UFMC [15]. As an alternative to OFDM and FBMC, UFMC has various advantages over OFDM and FBMC. [16, 17] Shows that UFMC has better spectral efficiency than FBMC. Similarly, UFMC is less implementation complexity than FBMC and reverse compatibility to older system. It is also implemented based on IFFT/FFT pairs and use prototype filter called Chebyshev which can decrease spectral leakage drawbacks of OFDM and FBMC systems. As we review current multiple access for LTE and their drawbacks to support a new application for future 5G. Another new candidate, which can be used in future 5G is UFMC. UFMC is a generalization of the advantage features of OFDM and FBMC [18]. In addition, it is avoid the drawbacks of the other two systems. It is operation based on filtering consecutive subband (a group of subcarriers) in modulation and demodulation. Some points of interests of UFMC are: It is a simple transceiver called UF-OFDM, with filtering length equal to 1 (L=1). The non-orthogonal carriers are not important, which means better spectral efficiency and low latency. Supporting 5G application like the internet of thing (IoT), M2M and D2D [19] which release strict synchronous transition between transmitter and receiver. V2V required a signal that is less sensitivity to CFO to achieve reliable communication between nodes mobile, Support M2M that require new physical interface and new media access control layer to ensure communication between machines to any like machine, human, vehicle. Another

978-1-5386-5697-6/18/$31.00 ©2018 IEEE
DOI 10.1109/ICPET.2018.00014

advantage is new signal design to allow different users to communicate at the same time in different subbands. Support the fragment spectrum and this allows sending small data packets. No CP, instead of that setting time of filter used as guard period. UFMC system is a generalization of combination advantages of current system OFDM and FBMC systems and avoided their limitations and restrictions. It is operation based in a filter of a consecutive subset of the complete band modulation and demodulation instead of filtering the whole band or single carrier.

Fading process estimation and equalization procedures are critical in a wireless communication system for symbol recovering bits at the receiver side. Transmitted signal is sensitive to many effects during traveling to the receiver.

Few UFMC studies have handle the issue of the channel estimation and equalization to the current date [20-22] compared to many studies were addressed in OFDM in the literature [23-26] and FBMC [27-30]. Channel estimation techniques in the UFMC and FBMC/OQAM are different in conventional techniques used in OFDM because the channel frequency response values are real in OFDM and complex in FBMC and UFMC. Second reason is subbands filtering operation for to decrease out of band emission (OOB) may produce dissimilar filter gain on different subcarriers for one UFMC symbol [31]. In [20] the author proposed estimation of UFMC channel in an uplink multiuser in timing and frequency offset and shows that the conventional pilot-aided channel estimation used in OFDM is efficient in UFMC. In [21] author introduces channel estimation based on combo type pilot pattern based on various algorithms like LSLI, DFT, and RMMSE. In [22] the authors introduce estimation using PRN to be as guard interval and TS at time domain to minimize total of transmitted pilots in the frequency domain and the effect will be improvement in spectral efficiency.

All proposed channel estimation techniques are categorized as blind techniques and training sequence/pilot based techniques. The advantage of the blind technique is no need to insert pilots, but the drawbacks are complexity and requiring a large amount of data and this means loss of efficiency. While the other technique is lower computational complexity.

In our research, we addressed pilot based technique. Many approaches were developed when using the Kalman filter for channel estimation [27] [32-34]. In [34] authors introduce the combination of Kalman filter with AR process to track channel variations achieving better results of BER performance than conventional adaptive estimators like LMS and RLS for MC-CDMA. While [32-33] describes the Kalman estimator with an AR model to estimation fading channel in OFDM. Recently, dual Kalman filters are proposed in [27] to estimate FBMC/OQAM fading channels process. The fading model performed by an AR, its coefficients are gained by (YWE).

The structure of this paper is formed as follows. We will introduce UFMC transceiver in section II. The estimation of fading process using AR model tracked by Kalman estimator in section III. Simulation and analyses results will be presented in section IV. Finally, The conclusion will be present in section V.

II. UFMC

In [35], the idea of UFMC system is presented in fig. (1.a). The operation of UFMC is filtering group of subband instead of filtering single carrier or whole band. To produce UFMC signal, every subbands carrying number of carriers convert to parallel and pass to IFFT block. After that, applying filtering operation to decrease OOB. The output of each filter was summed to form UFMC Signal. Moreover, since the number of a complex symbol in each subband is less than the IFFT points multiply with a number of subbands, the rest of block padded with number of zeros.

Mathematically, the information input to the UFMC system are complex of QAM symbol (s_k) is divided into subbands called B, k have the values of $(1 \dots N)$, Where "N" refers to IFFT constellation points. Each of subbands having numbers of subcarriers k and n_i of complex symbols. All subbands are padded with zeros carriers to make each block contain N symbols. Then converting frequency symbols $S_k = [S_{1k} \;\; S_{2k} \;\; S_{Bk}]$ to time domain $x = [x_{1K} \;\; x_{2K} \;\; x_{BK}]$ by using IFFT block. The result of each IFFT converted to serial. Each padded zero symbol is filtered with chebyshev window determined side lobe attenuation level and filter length L. Dolph-Chebyshev window have low sidelobe levels different from fixed window like Hanning windows. Forgiven sidelobe attenuation and filter length, Chebyshev window yield narrow main lobe compared to fixed window functions. The characteristics of the filter are shifted in frequency according to subcarriers for each subband. The output signal for each subband from each filter is added, and then transform to the frequency domain. The closed form of Chebyshev window can be express as follows:

$$W_{0,k} = \frac{\cos\left\{M\cos^{-1}\left[\beta\cos\left(\frac{\pi K}{M}\right)\right]\right\}}{\cosh\{M\cosh^{-1}(\beta)\}} \quad (1)$$

Where M denotes for IFFT points, *k=0, 1, 2....M-1*.

$\beta = \cosh[\frac{1}{M}\cosh^{-1}(10^{\alpha})]$, where α = (2, 3 ,4).The α parameters adjust the side lobe levels by the expression Side-lobe level in *dB*=-20α. For example, if, we have $\alpha = 3$ then the side-lobes level below the main-lobe with 60dB, where the main lobe peak normalize to zero. The chebyshev side lobes are called ripple in the stop band, comstellationsince they are equal in heights. The number of subbands B will be different according to according to application requirements. As example, if the UFMC system employed in fragmented spectrum then number of subbands equal to the accessible spectrum portion in the fragmented spectrum.

In other words, we have input data X that will be divided to B subband with k subcarriers. Each subband passing through IFFT block symbolized by matrix V. The result of IFFT block will be serialized and passing to filter represent with matrix F. We can express the baseband UFMC signal $x_k[n]$ by:

$$x_k[n] = \frac{1}{N}\sum_{i=1}^{B}\sum_{l=0}^{N+L-1}\sum_{m=1}^{N_i^{Sub}} X_i^m e^{j2\pi ml/N} f_{n-l} \quad (1)$$

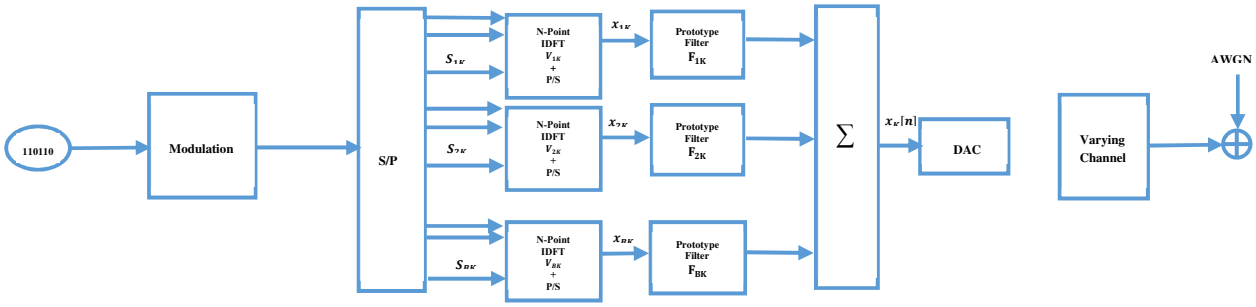

Figure 1.a: Block Diagram of UFMC Transmitter

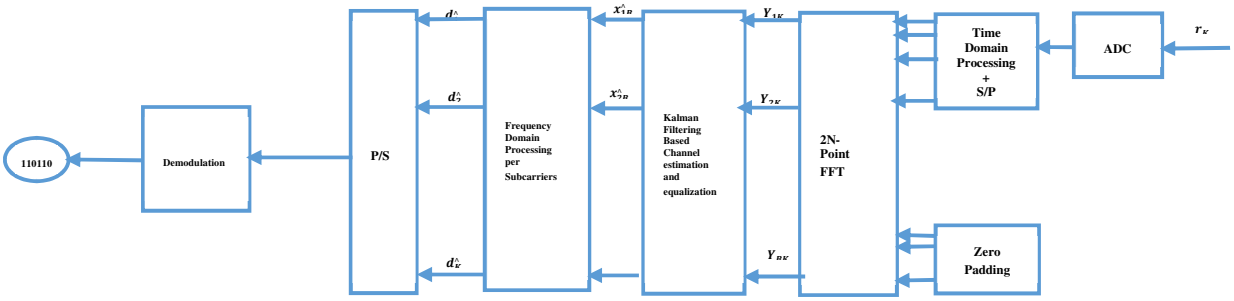

Figure 1.b: Block diagram of UFMC Receiver

Where N denotes for a number of FFT constellation points, while L denotes for the length of Chebyshev filter and f_{n-l} denotes for Chebyshev Filter.

UFMC has more elasticity for filtering every subband by its spectrum. It's can allow the scheme to adapt service types by regulating the subband and filter coefficients only. UFMC provide access for two different applications in the same time like M2M and D2D in two dissimilar subbands with disparate necessity and frame structure without creating inter-symbol band interference (ISBI) due to reduction OOB [22].

III. Kalman Filtering Based Channel Estimation

As we mentioned in section II, the delivered signal from the transmitter is transformed S/P and passed through FFT transformer block. The output of FFT serialize again then symbol demapper retrieve original data.

The received vector signal at the receiver after passing channel impulse response (CIR) can be represented by a transmitted signal $x_k[n]$ with the channel in addition to additive white Gaussian noise as in (2):

$$r_k[\mathrm{n}] = x_k[n]h_k[\mathrm{n}] + n_k[n] \tag{2}$$

By Substitution value of x in (2) we get:

$$r_k[\mathrm{n}] = h_k[\mathrm{n}]\frac{1}{N}\sum_{i=0}^{B}\sum_{l=0}^{N+L-1}\sum_{m=1}^{N_i^{Sub}} X_i^m e^{j2\pi ml/N} f_{n-l} + n_k[n] \tag{3}$$

Where h_k denotes for the complex-valued of fading process over k^{th} sub-band carriers for the m^{th} symbols and n_k denotes for AWGN process.

We assume the noise processes to be mutually (i.i.d) distributed zero-mean and variance ${\sigma_k}^2$. The fading process $h_k[n]$ can be Perform as a complex Gaussian process $h_k(n) = |h_k(n)|e^{-j\varphi_k(n)}$ with zero mean. With uniformly phase $\varphi_k(k)$ lying between [0,2π]. To utilize the statistical characteristics of fading signal, it is described the by PSD and zero order Bessel ACF. The PSD of fading signal represented by well-known *U* shaped band limited jakes spectrum with maximum Doppler frequency f_d [36].

$$\mathrm{S(f)} = \begin{cases} \dfrac{1}{\pi \mathrm{f_d}\sqrt{(\frac{\mathrm{f_d}-f}{\mathrm{f_d}})^2}}, & \text{for } \mathrm{f} \le |\mathrm{f_d}| \\ 0, & \text{Otherwise} \end{cases} \tag{4}$$

Where $f_d = \frac{v}{\lambda}$, with v light speed and λ, is the wavelength of wave carriers.

The Autocorrelation function (ACF) can be express by:

$$R_k = J_0(2\pi f_d T_s|k|) \tag{5}$$

Where J_0 denotes zero ordered Bessel function, T_s denote symbol period, and $f_d T_s$ point to Doppler rate. In [37] use general Autoregressive (AR) model to generate correlated Rayleigh processes with fading process that shape the spectrum of the uncorrelated Gaussian variates. Fading process can be designed by order of AR in [37]:

$$h[n] = -\sum_{k=1}^{p} a_k h[n-k] + \upsilon(n) \tag{6}$$

Where $\upsilon(n)$ refers to complex white Gaussian noise process with zero mean and driving process covariance ${\sigma_\upsilon}^2$. $\mathrm{a_k}$ denotes for the AR parameters. We can express the PSD of AR model by:

$$S(f_n) = \frac{\sigma_\upsilon^2}{\left|1+\sum_1^p a_i e^{(-j2\pi f_n i)}\right|^2} \tag{7}$$

Where f_n denotes the normalized frequency. $h_k(n)$ denotes fading process that estimated by the Kalman filter. The estimation of fading process $h_k(n)$ over the n^{th} along the carrier. The carrier subscript is dropped for simplicity and clarity, then the state vector can be express as follows:

$$\boldsymbol{h}_k = \left[\, h_k \;\; h_{k-1} \;\; \ldots h_{k-p+1} \,\right]^T \tag{8}$$

The expression (8) can be expressed as state space form as in follows:

$$\boldsymbol{h}_k = \boldsymbol{\phi}\boldsymbol{h}_{k-1} + \boldsymbol{g}\upsilon_k \tag{9}$$

Where:

$\boldsymbol{\phi} = \begin{bmatrix} -a_1 & -a_2 & \cdots & -a_p \\ 1 & 0 & \cdots & 0 \\ \vdots & \vdots & \ddots & \vdots \\ 0 & \cdots & 1 & 0 \end{bmatrix}$ Is the state transition model matrix and g express as in follows:

$$\boldsymbol{g} = [1\ 0\ \ldots 0]^T$$

In addition, by substation of equation (9) in equation (2), it follows:

$$r_k = \boldsymbol{x}_k^T \boldsymbol{h}_k + \eta_k \tag{10}$$

Where:

$$\boldsymbol{x}_k = [\, x_k \;\; 0 \;\cdots\; 0]^T \tag{11}$$

We will use a Kalman filter to estimate the fading process $\widehat{\boldsymbol{h}}_{k/k}$ for the state vector $\boldsymbol{h}_k$ by assumed a set of observations $\{r_i\}_{i=1,\cdots,k}$ are known. another process needed so-called innovation process α_k which refer to a difference between observed value and optimal value which can be obtained as follows:

$$\alpha_k = r_k - \boldsymbol{x}_k^T \boldsymbol{\phi} \widehat{\boldsymbol{h}}_{k-1/k-1} \tag{12}$$

The variance of the innovation process as follows:

$$C_k = E[\alpha_k \alpha_k^*] = \boldsymbol{x}_k^T \boldsymbol{P}_{k/k-1} \boldsymbol{x}_k + \sigma_{\eta_k}^2 \tag{13}$$

Where:

$\boldsymbol{P}_{k/\,k-1}$ represent a priori error covariance matrix that be get repetitively as follows:

$$\boldsymbol{P}_{k/k-1} = \boldsymbol{\phi}\boldsymbol{P}_{k/k-1}\boldsymbol{\phi}^H + \boldsymbol{g}{\sigma_\upsilon}^2 \boldsymbol{g}^T \tag{14}$$

The Kalman gain is enumerated by the next equation:

$$\boldsymbol{K}_k = \boldsymbol{P}_{k/k-1} \boldsymbol{x}_k C_k^{-1} \tag{15}$$

The estimation of a posteriori of fading process given by:

$$\widehat{\boldsymbol{h}}_{k/k} = \boldsymbol{\phi}\widehat{\boldsymbol{h}}_{k-1/k-1} + \boldsymbol{K}_k\, \alpha_k \tag{16}$$

And the state vector given by:

$$\hat{h}_k = \hat{h}_{k/k} = \boldsymbol{g}^T \widehat{\boldsymbol{h}}_{k/k} \tag{17}$$

The update of $\boldsymbol{P}_{k/k}$ is get repetitively as follows:

$$\boldsymbol{P}_{k/k} = \boldsymbol{P}_{k/k-1} - \boldsymbol{K}_k \boldsymbol{x}_k^T \boldsymbol{P}_{k/k-1} \tag{18}$$

We assign the initial value for the state vector $\widehat{\boldsymbol{h}}_{0/0}$ to zero vector i.e. $\widehat{\boldsymbol{h}}_{0/0} = 0$ and the initial value for the error covariance matrix $\boldsymbol{P}_{0/0}$ to identity matrix i.e. $\boldsymbol{P}_{0/0} = \boldsymbol{I}_p$

According to fig. (1.b), the received signal r_k passed to 2N-FFT block to tranform it into frequency domain, this block (2N-FFT) is very necessary for recovering symbols at *N* subcarriers from "$N + L - 1$" received samples. The result of FFT block transformer is given by:

$$Y(k) = \frac{1}{\sqrt{N}} \sum_{l=0}^{N+L-2} r_k[n]\, e^{-j2\pi lk/2N}, k = 0,1\ldots 2N-1 \tag{19}$$

Channel equalizing is estimated using multiplying received signal with normalize version of the complex conjugate of the channel estimate as:

$$\hat{x}_k(n) = Y_k(n) \left(\frac{\hat{h}_k^*(n)}{|\hat{h}_k(n)|^2} \right) \tag{20}$$

IV. Simulation Results

In this part, we will estimate high varying fading channel process between conventional filters like LMS, RLS and our proposed estimator Kalman filter combined with the autoregressive model with comb pilot arrangement 1:8. In addition, we will compare power spectral density between three modulation system OFDM, FBMC and UFMC.

Fig. (2) shows the BER performance of UFMC using different mapping techniques. It is clear that the best QAM modulation when we use the Bits per subcarrier (M=4).

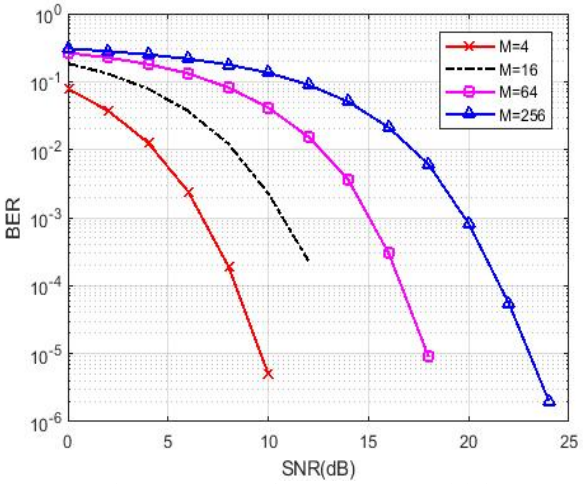

Fig.2: BER vs SNR for UFMC QAM Modulation

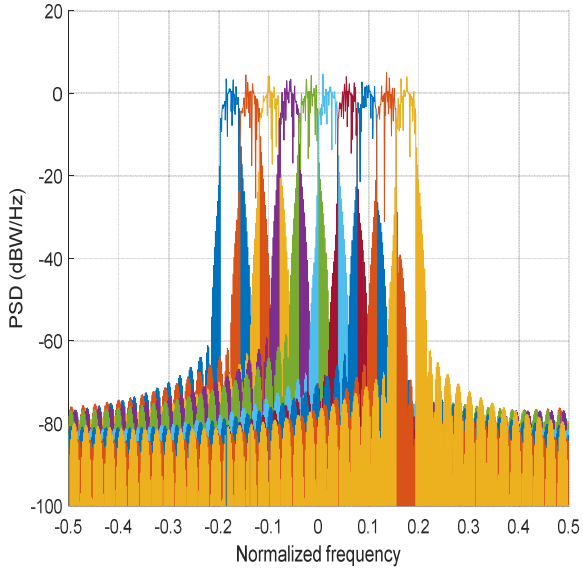

Fig.3: PSD vs Normalize frequency for UFMC, 10 Subband, 20 Subcarriers for each

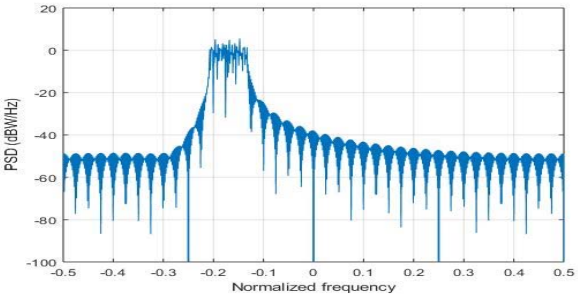

Fig. 4: PSD vs Normalize frequency Power for OFDM, 200 Subcarriers

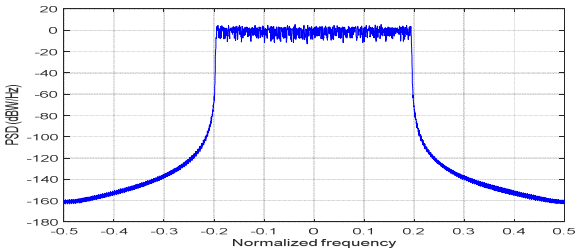

Fig. 5: PSD vs Normalize frequency Power for FBMC, 200 Subcarriers, Overlapped symbols K=4

Fig. (3), Fig. (4) and Fig. (5) illustrate respectively the PSD performance for the same number of subcarriers (200 Subcarriers) for UFMC, OFDM, and FBMC respectively. The PSD for candidate multiple access UFMC is higher than the rest Candidate system.

Given Fig. (6) that shows the envelope of an estimated fading channel generated by Rayleigh fading model with Doppler rate, $f_d T_s = 0.0185$.

According to Fig. (7), it illustrates the BER performance for Kalman estimator in addition to LMS, RLS for higher Doppler rate $f_d T_s = 0.0556, \mathrm{v} = 150\mathrm{km/h}$. It is notable that the performance of the Kalman estimator has lower BER.

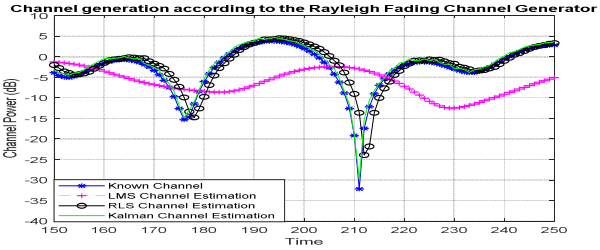

Fig 6: Channel Generation according to Rayleigh Fading Generator, $\boldsymbol{f_d T_s} = \mathbf{0.0185}$, μ=0.03, λ=0.4

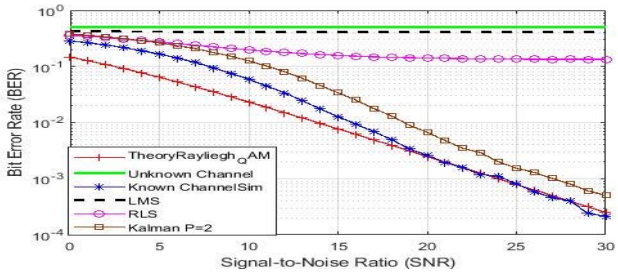

Figure 7: BER vs SNR for UFMC System, $\boldsymbol{f_d T_s} = \mathbf{0.0556}$

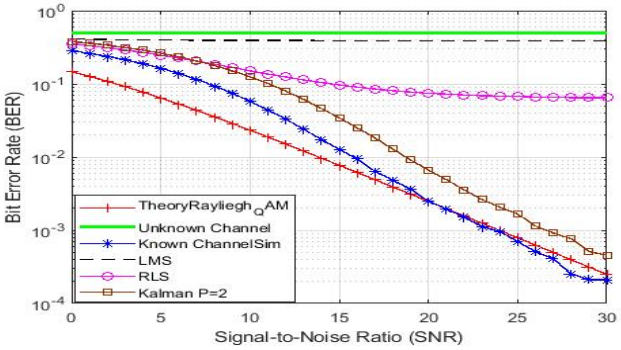

Figure 8: BER vs SNR for UFMC System, $\boldsymbol{f_d T_s} = \mathbf{0.0259}$

BER performance for Doppler rate $f_d T_s = 0.0259$ in Fig. (8), The BER performance for the Kalman estimator is better than the other estimators. Also, we notice improvement of BER for RLS estimator for the same scenario (Doppler rate smaller than the Doppler rate in Fig. (7).

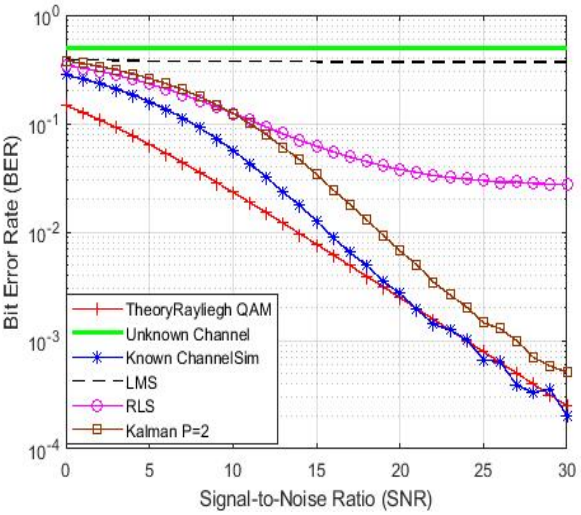

Figure 9: BER vs SNR for UFMC System, $\boldsymbol{f_d T_s} = \mathbf{0.0185}$

The Simulation results in Fig. (9). BER performance for low Doppler rate $f_d T_s = 0.0185$, Kalman estimator is still the best among the others. Also, we notice BER performance improvement for RLS estimator for lower Doppler rate.

VI. Conclusions

Current multiple access used in LTE is not a candidate for future mobile generation dues to their limitations and restrictions. After comparative between various candidate systems, the UFMC system has a strong candidate for later mobile generation 5G. In this research, we address the estimation and equalization of the UFMC fading channel by Kalman filter combined with the autoregressive process. The simulation results show that the Kalman filter overcomes performance conventional filter like LMS, RLS, and shows the performance of UFMC cope the performance of current system used in current 4G.

REFERENCES

[1] Li, Ye Geoffrey, and Gordon L. Stuber, eds. orthogonal frequency division multiplexing for wireless communications. Springer Science & Business Media, 2006.

[2] K. Baum, Kevin, Brian Classon, and Phillire Sartori. Principles of broadband OFDM cellular system design. Wiley, 2008.

[3] Farhang-Boroujeny, Behrouz. "OFDM versus filter bank multicarrier." IEEE signal processing magazine 28, no. 3 (2011): 92-112.

[4] H Zhang, Haijian, Didier Le Ruyet, Daniel Roviras, Yahia Medjahdi, and Hong Sun. "Spectral efficiency comparison of OFDM/FBMC for uplink cognitive radio networks." EURASIP Journal on Advances in Signal Processing 2010 (2010): 4.

[5] G.Bochechka. "Methods of channel estimation based on built in pilot-signals in OFDM systems". Telecommunications and Transport, 2009, No3, pp. 38-42.

[6] G. Bochechka, Estimation of the beginning of the OFDM block and frequency shift in system IEEE 802.11a.T-Comm Telecommunications and Transport, 2009, №5, pp.34-37.

[7] F.Hu, "Opportunities in 5G Networks a research and development perspective", CRC Press,2016

[8] Cisco,https://www.cisco.com/c/en/us/solutions/collateral/service-provider/visual-networking-index-vni/mobile-white-paper-c11-520862.html

[9] Tullberg, Hugo, Heinz Droste, Mikael Fallgren, Peter Fertl, David Gozalvez-Serrano, Eiman Mohyeldin, Olav Queseth, and Yngve Seien. "METIS research and standardization: A path towards a 5G system." In Globecom Workshops (GC Wkshps), 2014, pp. 577-582. IEEE, 2014.

[10] ''More than 50 billion connected devices,'' Ericsson, Stockholm, Sweden, White Paper 284 23-3149, Feb. 2011. [Online]. Available:

[11] http://www.akos-rs.si/files/Telekomunikacije/Digitalna_agenda/Internetni_protokol_Ipv6/More-than-50-billion-connected-devices.pdf

[12] Wunder, Gerhard, Peter Jung, Martin Kasparick, Thorsten Wild, Frank Schaich, Yejian Chen, Stephan Ten Brink et al. "5GNOW: non-orthogonal, asynchronous waveforms for future mobile applications." IEEE Communications Magazine 52, no. 2 (2014): 97-105.

[13] Schaich, Frank, and Thorsten Wild. "Waveform contenders for 5G—OFDM vs. FBMC vs. UFMC." In Communications, Control and Signal Processing (ISCCSP), 2014 6th International Symposium on, pp. 457-460. IEEE, 2014.

[14] Farhang-Boroujeny, Behrouz. "OFDM versus filter bank multicarrier." IEEE signal processing magazine 28, no. 3 (2011): 92-112.

[15] G. Fettweis, Gerhard, Marco Krondorf, and Steffen Bittner. "GFDM-generalized frequency division multiplexing." In Vehicular Technology Conference, 2009. VTC Spring 2009. IEEE 69th, pp. 1-4. IEEE, 2009.

[16] Vakilian, Vida, Thorsten Wild, Frank Schaich, Stephan ten Brink, and Jean-Francois Frigon. "Universal-filtered multi-carrier technique for wireless systems beyond LTE." In Globecom Workshops (GC Wkshps), 2013 IEEE, pp. 223-228. IEEE, 2013.

[17] F. Schaich, Frank, Thorsten Wild, and Yejian Chen. "Waveform contenders for 5G-suitability for short packet and low latency transmissions." In Vehicular Technology Conference (VTC Spring), 2014 IEEE 79th, pp. 1-5. IEEE, 2014.

[18] Gerzaguet, Robin, Nikolaos Bartzoudis, Leonardo Gomes Baltar, Vincent Berg, Jean-Baptiste Doré, Dimitri Kténas, Oriol Font-Bach et al. "The 5G candidate waveform race: a comparison of complexity and performance." EURASIP Journal on Wireless Communications and Networking 2017, no. 1 (2017): 13.

[19] Wang, Xiaojie, Thorsten Wild, Frank Schaich, and A. Fonseca Dos Santos. "Universal filtered multi-carrier with leakage-based filter optimization." In European Wireless Conference, pp. 1-5. 2014.

[20] Duan, Sirui, Xiang Yu, and Rong Wang. "Performance Analysis on Filter Parameters and Sub-bands Distribution of Universal Filtered Multi-Carrier." Wireless Personal Communications 95, no. 3 (2017): 2359-2375.

[21] Wang, Xiaojie, Thorsten Wild, Frank Schaich, and Stephan ten Brink. "Pilot-aided channel estimation for universal filtered multi-carrier." In Vehicular Technology Conference (VTC Fall), 2015 IEEE 82nd, pp. 1-5. IEEE, 2015.

[22] Zhang, Lei, Chang He, Juquan Mao, Ayesha Ijaz, and Pei Xiao. "Channel estimation and optimal pilot signals for universal filtered multi-carrier (UFMC) systems." In Personal, Indoor, and Mobile Radio Communications (PIMRC), 2017 IEEE 28th Annual International Symposium on, pp. 1-6. IEEE, 2017.

[23] Wang, Rong, Jingye Cai, Xiang Yu, and Sirui Duan. "Compressive channel estimation for universal filtered multi-carrier system in high-speed scenarios." IET Communications 11, no. 15 (2017): 2274-2281.

[24] Ozdemir, Mehmet Kemal, and Huseyin Arslan. "Channel estimation for wireless OFDM systems." IEEE Communications Surveys & Tutorials 9, no. 2 (2007): 18-48.

[25] Coleri, Sinem, Mustafa Ergen, Anuj Puri, and Ahmad Bahai. "Channel estimation techniques based on pilot arrangement in OFDM systems." IEEE Transactions on broadcasting 48, no. 3 (2002): 223-229.

[26] Manton, Jonathan H. "Optimal training sequences and pilot tones for OFDM systems." IEEE Communications Letters 5, no. 4 (2001): 151-153.

[27] Lin, Jia-Chin. "Least-squares channel estimation for mobile OFDM communication on time-varying frequency-selective fading channels." variations 4, no. 6 (2008): 12.

[28] Aldababseh, Mahmoud, and Ali Jamoos. "Estimation of FBMC/OQAM fading channels using dual Kalman filters." The Scientific World Journal 2014 (2014).

[29] Kofidis, Eleftherios, Dimitrios Katselis, Athanasios Rontogiannis, and Sergios Theodoridis. "Preamble-based channel estimation in OFDM/OQAM systems: A review." Signal Processing 93, no. 7 (2013): 2038-2054.

[30] Kofidis, Eleftherios, and Dimitrios Katselis. "Improved interference approximation method for preamble-based channel estimation in FBMC/OQAM." In Signal Processing Conference, 2011 19th European, pp. 1603-1607. IEEE, 2011.

[31] Chen, Chih-Wei, and Fumiaki Maehara. "An enhanced MMSE subchannel decision feedback equalizer with ICI suppression for FBMC/OQAM systems." In Computing, Networking and Communications (ICNC), 2017 International Conference on, pp. 1041-1045. IEEE, 2017

[32] Zhang, Lei, Ayesha Ijaz, Pei Xiao, Muhammad Ali Imran, and Rahim Tafazolli. "MU-UFMC system performance analysis and optimal filter length and zero padding length design." arXiv preprint arXiv:1603.09169 (2016).

[33] W. Chen and R. Zhang, "Estimation of time and frequency selective channels in OFDM systems: a Kalman filter structure," in Proc. IEEE GLOBECOM'04, pp. 800-803, Nov. 2004.

[34] Jamoos, Ali, Ahmad Abdo, and Hanna Abdel Nour. "Estimation of OFDM time-varying fading channels based on two-cross-coupled Kalman filters." In Novel Algorithms and Techniques in Telecommunications, Automation and Industrial Electronics, pp. 287-292. Springer, Dordrecht, 2008.

[35] Kalofonos, Dimitris N., Milica Stojanovic, and John G. Proakis. "Performance of adaptive MC-CDMA detectors in rapidly fading Rayleigh channels." IEEE Transactions on Wireless Communications 2, no. 2 (2003): 229-239.

[36] Bochechka, Grigory, Valery Tikhvinskiy, Ivan Vorozhishchev, Altay Aitmagambetov, and Bolat Nurgozhin. "Comparative analysis of UFMC technology in 5G networks." In Control and Communications (SIBCON), 2017 International Siberian Conference on, pp. 1-6. IEEE, 2017.

[37] WC Jr, Jakes. "Microwave mobile communications." (1974).

[38] Baddour, Kareem E., and Norman C. Beaulieu. "Autoregressive modeling for fading channel simulation." IEEE Transactions on Wireless Communications 4, no. 4 (2005): 1650-1662.